Combining spectroscopy and magnetism with geochemical tracers to improve the discrimination of sediment sources in a homogeneous subtropical catchment

Rafael Ramon, Olivier Evrard, J. Patrick Laceby, Laurent Caner, Alberto Inda, Cláudia A.P. De Barros, Jean P.G. Minella, Tales Tiecher

Combining spectroscopy and magnetism with geochemical tracers to improve the discrimination of sediment sources in a homogeneous subtropical catchment

Rafael Ramon[a,b]; Olivier Evrard[b]; J. Patrick Laceby[c]; Laurent Caner[d], Alberto V. Inda[e], Cláudia A.P. de Barros[e]; Jean P.G. Minella[f] and Tales Tiecher[e]

[a] Graduate Program in Soil Science, Federal University of Rio Grande do Sul, Bento Gonçalves Ave., 91540-000 Porto Alegre, RS, Brazil – Interdisciplinary Research Group On Environmental Biogeochemistry - IRGEB (rafaramon11@gmail.com)

[b] Laboratoire des Sciences et de l'Environnement, UMR 8212 (CEA/CNRS/UVSQ), 91 191 Gif-sur-Yvette Cedex (France), Université Paris-Saclay, France – IRGEB (olivier.evrard@lsce.ipsl.fr)

[c] Alberta Environment and Parks, 3535 Research Rd NW, T2L 2K8, Calgary, Alberta, Canada (patrick.Laceby@gov.ab.ca)

[d] IC2MP-HydrASA UMR, Université de Poitiers, Poitiers, France (laurent.caner@univ-poitiers.fr)

[e] Department of Soil Science, Federal University of Rio Grande do Sul, Bento Gonçalves Ave. 7712, 91540-000 Porto Alegre, RS, Brazil – IRGEB (alberto.inda@ufrgs.br; claudia.barros@ufrgs.br; tales.tiecher@gmail.com)

[f] Department of Soil Science, Federal University of Santa Maria, Roraima Ave. 1000, 97105-900 Santa Maria, RS, Brazil – IRGEB (jminella@gmail.com)

Abstract

An important step in the sediment source fingerprinting approach is the selection of the appropriate tracing parameters to maximize source discrimination. The use of multiple tracing properties may reduce uncertainties and increase discrimination between sources. Accordingly, this study investigates the discrimination and quantifies the contribution of sediment sources delivering sediment to a river draining a homogeneous subtropical agricultural catchment based on the combination of ultraviolet-visible spectra derived parameters (UV), magnetic (M), and geochemical tracers (GEO). The investigated catchment (Conceição River - 804 km^2), located in Southern Brazil, has predominantly deep and strongly weathered Ferralsols. The main land-uses found in the area are cropland (89%), pasture (5%) and forest (5%). A total of 187 samples were collected to characterise the five main sediment sources, including cropland, pastures, unpaved roads, gullies and stream banks. A total of 53 tracers, including 21 geochemical tracers, two magnetic properties and 30 parameters derived from UV spectra, were analysed. Tracers were selected following a three step procedure, including: (i) an interquartile range test, (ii) a Kruskal–Wallis H test, and (iii) a linear discriminant function analysis (LDA). The LDA was performed using six different sets of variables: (i) GEO only; (ii) UV only; (iii) M+UV (MUV); (iv) GEO+UV (GUV); (v) GEO + M (GM) and (vi) GEO+M+UV (GMUV). The selected tracers were introduced into a mass balance mixing model to estimate the source contributions to in-stream sediment by minimizing the sum of square residuals. Most geochemical tracers were considered not conservative by using the interquartile range test in this catchment with highly weathered soils. The GM approach resulted in the highest percentage of samples correctly classified (SCC), with 74%, followed by the approaches with GMUV and GUV, with 73%. Alternative tracers, UV individually or combined with M tracers,

47 correctly classified only 59 and 60% of the samples, respectively. Moreover, they did
48 not provide significant additional discrimination power even when combined with the
49 GEO tracers. The apportionment model resulted in similar source contribution results
50 for all approaches, with the absence of significant difference when comparing the mean
51 source contributions obtained for the entire set of sediment samples (Cropland: 17–
52 23%; Pastures: 24–34%; Unpaved Roads: 3–12%; Stream Banks: 26–31%; Gullies: 14–
53 19%). Due to the strong homogeneity of soil types found in the Conceição catchment,
54 these differences in source contributions remained very low and the results of the
55 mixing model were impacted by the high number of potential sources and the relatively
56 limited quality of the sediment source discrimination. According to the model results,
57 the low discrimination between the potential sediment sources illustrates the
58 difficulties for discriminating land-used based sediment sources, with more than three
59 potential sources, in homogeneous catchments with highly weathered soils (e.g.
60 Ferralsols, Nitisols) under tropical conditions.
61

Highlights

- Geochemical tracers were not conservative in a catchment with highly weathered soils.
- Magnetic and UV tracers had low discriminating potential between land uses.
- The low discrimination between sources results in great uncertainties in the results.
- Quantifying sediment contributions from more than three sources remains challenging.
- Despite limited discrimination, results of all tracers combinations remained consistent.

Key Words

Sediment fingerprinting; soil erosion; composite fingerprinting, tracer selection, geochemistry.

1 Introduction

The sustainable production of food, fiber and fuel remains limited by soil erosion. Despite the vast knowledge accumulated about soil erosion, it remains a significant global environmental issue that is one of the main causes of soil degradation worldwide. In this context, Southern Brazil has one of the highest erosion rates in the world (Borrelli et al., 2017) due to the relief characteristics along with intense and erosive rainfall (Ramon et al. 2017). In particular, rainfall erosivity is expected to increase ~10% in Southern Brazil by 2040 (Almagro et al., 2017).

Although field research programs are an essential tool to understand the impacts of human activities and climate changes on natural resources (Poesen, 2017), in Brazil they have been employed only relatively recently compared to other regions of the world such as the United States or Europe (Melo et al., 2020). In this scenario of limited hydrological and geomorphological understanding, it is important to identify the main sediment sources (Collins et.al, 2017) to guide decision-makers in the efficient allocation of limited public resources available to mitigate soil erosion and sediment production.

The sediment fingerprinting technique has been increasingly used in catchments worldwide to quantify the relative source contributions to river sediment (Walling, 2013). The method offers an effective way to calculate the contribution of diffuse sources of sediment and contaminants, providing useful information to focus efforts on controlling major soil erosion problems (Niu et al., 2019; Nosrati and Collins, 2019; Torres Astorga et al., 2018; Uber et al., 2019). However, many challenges require further research with sediment source fingerprinting such as the selection of tracers to

97 analyse and the grouping of the main sediment sources (Pulley et al., 2017b; Smith et al.,
98 2015).

99 Sediment tracer properties need to be conservative and their signature from
100 source to the river network must remain constant or vary predictably (Belmont et al.,
101 2014; Laceby et al., 2017). Although it is known that the conservativeness of potential
102 inorganic tracers is dependent on their chemical nature (e.g., alkali metals, transition
103 metals, rare earth elements) and how they are bound to the sediment (e.g., sorbed onto
104 sediment particles or matrix-bounded elements), there is still no consensus on the best
105 approach to assess conservativeness.

106 Most studies typically evaluate conservativeness empirically through
107 comparisons of concentration between sources and sediments, which in turns depend
108 on the conservativeness test applied (Smith et al., 2018; Lizaga et al., 2020). Moreover,
109 tracer conservativeness can also be dependent on the characteristics of the studied
110 catchment and the sediment sources evaluated. Studying land use sources in
111 homogeneous catchments may be much more challenging as any enrichment or
112 depletion of a particular element during the erosion process can result in sediment
113 concentrations varying outside the range of source values (Smith and Blake, 2014). To
114 overcome conservativeness issues and increase the number of conservative tracers,
115 physical characteristics such as colour, or related to mineralogical constitution, such as
116 magnetism and parameters related to Fe oxides, that can be easily measured, may
117 potentially maintain their conservativeness in these homogeneous catchments and be
118 combined with other tracing parameters (Pulley et al., 2018).

119 In addition, tracer properties should ideally be low-cost, quick and easy to
120 analyse, as characterizing a large number of samples is needed in order to be
121 representative of the within-source variability, especially in large catchments.

122 Furthermore, analyses that require a low sample mass and are non-destructive are
123 preferable, as in several environmental contexts, it can be difficult to collect large
124 quantities of suspended sediment during fieldwork (Guzmán et al., 2013).

125 Geochemical composition of source and sediment samples is among the most
126 used tracers for sediment fingerprinting worldwide (Koiter et al., 2013). Multiple
127 geochemical analyses such as inductively coupled plasma (ICP) or X-ray fluorescence
128 analyses result in high number of potential tracers, however they are not an option for
129 research groups that do not have access to sophisticated equipment (e.g. ICP-OES or
130 ICP-MS, microwave oven) or sufficient resources to afford such analysis.

131 Another option for tracing sediment sources are magnetic properties which have
132 been widely used since the original sediment fingerprinting studies (Walling et al.,
133 1979; Yu and Oldfield, 1989). Some measures like magnetic susceptibility can be easily
134 measured with relatively basic equipment (Rowntree et al., 2017), increasing the
135 number of tracers available for multiple sources contribution apportionment.

136 Moreover, spectroscopy data have been intensively investigated in the last
137 decade as a low-cost, non-destructive and straightforward alternative method to
138 provide tracer properties (Poulenard et al, 2009; Pulley et al., 2018). A variety of
139 approaches have been used to incorporate spectroscopy analysis into sediment
140 fingerprinting research (Legout et al., 2013; Martínez-Carreras et al., 2010b; Poulenard
141 et al., 2012; Tiecher et al., 2017). Among them, the use of colour parameters and
142 spectral features derived from ultraviolet-visible (UV) has shown to be promising
143 because it can be used alone or incorporated into mathematical models together with
144 geochemical tracers, radionuclides and others (Brosinsky et al., 2014a, 2014b, Tiecher
145 et al., 2015). Ultra-violet derived parameters may therefore offer a strong potential for

146 sediment tracing, although the proper classification of sources and the use of effective
147 modelling strategies are required to obtain reliable results (Pulley et al., 2018).

148 An important question in sediment fingerprinting surrounds the proper
149 identification of the potential sources of sediment to be incorporated into end-member
150 mixing models. Reducing the number of sources considered based on their relevance in
151 the study sites, or regrouping similar sources is a common practice in sediment
152 fingerprinting studies. For instance, Pulley et al. (2015b) did not consider grassland as a
153 source, since it occupied only a very low proportion of the catchment area and because
154 it was not possible to discriminate between cultivated and grassland areas with the
155 tracers used. A similar decision was taken by Minella et al. (2004), where fallow areas
156 could not be distinguished from pasture by the geochemical tracers used, and then they
157 were combined, while channel banks and new fields were removed because there was
158 not enough data to discriminate them, reducing the previous six sources to three.

159 In a previous study conducted in the Conceição River catchment in Southern
160 Brazil, pastures were not considered as potential sources, since the geochemical tracers
161 were not able to discriminate pastures from croplands and because they occupy only a
162 low percentage of the total catchment surface area (Tiecher et al., 2018). Gullies were
163 also not considered, as they are not commonly observed in the Conceição catchment,
164 where rill erosion is much more widespread (Didoné et al., 2015). In this catchment,
165 which consists of relatively homogeneous soil and geology, geochemical tracers were
166 only able to correctly classify only 84% of the samples in their respective source groups
167 (ie., cultivated sources, unpaved roads and streambanks) (Tiecher et al., 2018). The
168 small difference in the elemental concentrations observed between the sources, because
169 of intense weathering and leaching of most elements except Al and Fe, complicated their

discrimination, requiring further studies and alternative tracers to increase the robustness of the results.

Here, the use of low-cost alternative parameters, including spectroscopy derivatives in the ultraviolet-visible range and magnetic parameters, in combination with geochemical tracers are investigated to provide an alternative approach that increases the discrimination between multiple land use sources. This research investigates the potential of six different sets of tracing parameters combing low cost and geochemical element traces to calculate the respective contributions of five potential sediment sources in a homogeneous catchment (Conceição River) in southern Brazil. This research contributes to the ongoing development of low-cost tracers, examining their efficacy in a complicated homogeneous tracing environment, that is representative of regions with extensive agricultural activities that contribute deleterious sediment loads degrading waterways worldwide.

2 Methodology

2.1 Study site

The Conceição River catchment is located on a basaltic plateau in the southern part of the Paraná Basin in the state of Rio Grande do Sul, and it covers an area of approximately 804 km^2 (Figure 1). According to Köppen's classification, the climate is classified as of Cfa type, humid subtropical without a defined dry season, with an average annual precipitation ranging between 1750 to 2000 mm per year and an average temperature of 18.6°C. This catchment is representative of the basaltic plateau region of the Serra Geral Formation (92%), where the soil classes found are Ferralsols (80%), Nitisols (18%) and Acrisols (2%), with a mineralogy dominated by iron oxides

and kaolinite (Figure 2). These soils are very rich in clays, typically, the Ferralsols that predominate in this catchment have less than 10% of sand and clay content as high as 85% (Ramos et al., 2017). Small areas from the Tupanciretã Formation (6%), which are outcrops of the Botucatu Formation enclosed by volcanic spills of the Serra Geral Formation, are also found. The relief of the catchment is characterized by gentle slopes (6-9%) at the higher positions of the landscape and steeper slopes (10-14%) near the drainage channels, with altitudes ranging from 270 to 480 m a.s.l. The catchment outlet is located next to the monitoring point number 75200000 of the National Water Agency (ANA) (28°27'22" S, 53°58'24" O) in the municipality of Ijuí.

The main land use is cropland (89%) mainly cultivated with soybean (*Glycine max*) under no tillage system in the summer and with wheat (*Triticum aestivum*) for grain production, oat (*Avena sativa* and *Avena strigosa*) and ryegrass (*Lolium multiflorum*) for dairy cattle feed or used as cover crops for protecting the soils during winter. However, inadequate soil management in these areas, without crop rotation, cover crops during the autumn and winter, and mechanical practices to control surface runoff, has resulted in high erosion rates during the last 60 years, even with the no-tillage system implemented during the last 30 years (Didoné et al., 2019, 2015). Grasslands and pasture, mainly used for cattle raising, cover 5% of the total surface area, whereas forest is found on only 5% of the surface. Approximately 1 to 2% of the area is occupied by non-vegetated areas, urban infrastructure and water bodies.

2.2 Source and sediment sampling

Soil composite samples (n=187) were collected in areas representative of the potential sediment sources, which include cropland (n=77), pasture (which include grasslands and permanent pastures, n=24), unpaved road (n=38), stream bank (n=34) and gullies (n=14) (Figure 2). The source samples were taken from the surface layer (0

– 5 cm) of cropland and pasture (surface sources). In gully sites and stream bank samples were taken from the exposed sidewall avoiding the material of the most superficial layer (0-5 cm). The height exposed in the gullies sites and stream banks varies greatly, but as the soil below the surface layer is quite homogeneous in the Ferralsols of this catchment, the samples were collected in a representative manner throughout the exposed subsurface area. To characterize unpaved roads, samples were taken mainly in the roadsides where erosion is more evident, which in all cases correspond to the subsurface of the soil, always avoiding collecting transient materials from other potential sources. Care was taken to avoid those sites that have accumulated sediment originating from other sources. Around ten sub-samples were collected within a radius of approximately 50 m and mixed to prepare a composite sample, in order to obtain representative source material. Samples were taken at sites sensitive to erosion and connected to the stream network, and attention was paid to cover all the range of soil types found in the catchment.

Eleven sediment samples were collected at the catchment outlet during the monitoring period (Appendix A). From these, eight samples are fine-bed sediment (FBS) collected in the bottom of the river with a suction device and three samples were collected with a time-integrated sediment sampler (TISS) designed according to Phillips et al. (2000). The period during which the TISS was sampled and the collection date of each FBS sample are detailed in Table 1.

2.3 Source and sediment analyses

All samples were oven-dried (50°C), gently disaggregated using a pestle and mortar and dry-sieved to 63 μm to avoid particle size effects prior to further analysis (Koiter et al., 2013; Laceby et al., 2017).

2.3.1 Geochemical properties

A total of 20 geochemical elements were evaluated as potential tracers. The total concentration of Al, Ba, Be, Ca, Co, Cr, Cu, Fe, K, La, Li, Mg, Mn, Na, Ni, P, Sr, Ti, V, and Zn was determined using inductively coupled plasma optical emission spectrometry (ICP-OES) after microwave-assisted digestion with concentrated HCl and HNO_3 (ratio 3:1) for 9.5 min at 182 °C. This method was adapted from U.S. EPA (2007), as it was reported to provide satisfactory recovery for quantifying metal concentrations in soils (Chen and Ma, 2001; Da Silva et al., 2014). Total organic carbon (TOC), which was estimated by wet oxidation ($K_2Cr_2O_7$ + H_2SO_4 - Walkley and Black, 1934), was included in the set of geochemical tracers.

2.3.2 Magnetic properties

Two grams of each sample were used to measure the magnetic susceptibility in a Bartington MS2B Dual Frequency sensor, with three readings for each sample at high (4.7 kHz) and low frequencies (0.47 kHz) to obtain the mass specific magnetic susceptibility for high (χ_{HF} – m^3 kg^{-1}) and low frequencies (χ_{LF} – m^3 kg^{-1}) (Mullins, 1977).

2.3.3 Ultraviolet-visible analysis and parameters calculation

The diffuse reflectance spectra in the ultraviolet-visible (UV) wavelengths (200 to 800 nm, with 1 nm step) were measured for each powdered sample using a Cary 5000 UV-NIR spectrophotometer (Varian, Palo Alto, CA, USA) at room temperature, using $BaSO_4$ as 100% reflectance standard. Twenty-two colour parameters were derived from the UV spectra following the colorimetric models described in details by Viscarra Rossel et al. (2006), which are based on the Munsell HVC, RGB, the decorrelation of RGB data, CIELAB and CIELUV Cartesian coordinate systems, three parameters from the HunterLab colour space model (HunterLab, 2015) and two indices

(coloration – CI and saturation index – SI) (Pulley et al., 2018). In total, 27 colour metric parameters were derived from the spectra of source and sediment samples (L, L*, a, a*, b, b*, C*, h, RI, x, y, z, u*, v*, u', v', Hvc, hVc, hvC, R, G, B, HRGB, IRGB, SRGB, CI and SI). Three other parameters were calculated from the second derivative curves of remission functions in the visible range of soil and sediment samples, which displayed three major absorption bands at short wavelengths commonly assigned to Fe-oxides (Caner et al., 2011; Fritsch et al., 2005; Kosmas et al., 1984; Scheinost et al., 1998) (Appendix B).

2.4 Sediment source discrimination and apportionment

The selection of the discriminant tracers followed the classical three-step procedure, including: i) a range test; ii) the Kruskal-Wallis *H* test (KW *H* test); and iii) a linear discriminant function analysis (LDA) (Collins et al., 2010a). In the range test, variables with median ± the interquartile range (IQR, 25^{th} and 75^{th} percentiles) values of sediment samples lying outside the range of the sources were excluded (Batista et al., 2018). The KW *H* test was performed to test the null hypothesis ($p < 0.05$) that the sources belong to the same population. The variables that provided significant discrimination between sources were analysed with a forward stepwise LDA ($p < 0.1$) in order to reduce the number of variables to a minimum that maximizes source discrimination (Collins et al., 2010b). The statistical analyses were performed with R software (R Development Core Team, 2017) and more details can be found in Batista et al. (2018).

The source contributions were estimated by minimizing the sum of squared residuals (SSR) of the mass balance un-mixing model. Optimization constraints were set to ensure that source contributions were non-negative and that their sum equalled 1. The un-mixing model was solved by a Monte Carlo simulation with 2500 iterations. More information about model settings and compilation can be found in Batista et al.

(2018). Model uncertainties were evaluated based on the interquartile variation range of the predictions from the multiple interactions of the Monte Carlo simulation. The standard deviation (SD) of the Monte Carlo simulation results is calculated for each sediment sample and source.

In order to test the ability of magnetic (M) and ultraviolet-visible derived variables (UV) to discriminate between sediment sources, six approaches were tested to verify the contribution of each variable dataset. A first approach was carried out considering only geochemical variables (GEO) as potential tracers and the LDA and apportionment model results were compared to those obtained with geochemical tracers combined with M variables (GM), GEO plus UV (GUV), all variables together (GMUV) and UV variables alone. Finally, an approach was carried out considering only those "alternative" variables, involving M plus UV derived parameters (MUV).

3 Results

3.1 Selection of sediment tracers

All parameters were analysed individually to check their conservative behaviour and the property distribution in each group was evaluated using box plots. The interquartile range was more restrictive than the classical range test based on maximum and minimum values measured in the sources, resulting in a high number of tracers (70 %) removed by the range test (Table 2). From the 21 geochemical elements, only five behave conservatively (TOC, Be, Fe, K and P) . The set of 30 UV parameters included nine conservative properties (L*, x, L, a, b, v*, v', hVc, and B). Magnetic parameters, χ_{HF} and χ_{LF} were both conservative. It means that about 24, 30 and 100% of geochemical, UV parameters and magnetism tracers, respectively, behaved conservatively when applied the IQR range test. If applied the classical range test, about

317 72, 97 and 100% of geochemical, UV parameters and magnetic tracers, respectively,
318 behaved conservatively.

319 The KW H test was applied to all tracers, even to those that were not retained by
320 the conservativity test. Only five tracers did not hold potential to discriminate between
321 at least two potential sources (Cu, Ni, Fe, Na and A2 had $p > 0.1$) (Table 4). Among the
322 parameters that were conservative and passed the KW H test, the combination of
323 tracers that best discriminated between the sources was selected by the LDA, which are
324 presented in Table 3.

325 When geochemical data were used as potential tracers, P, K and TOC were
326 always selected as tracers. TOC and P are well correlated (Figure 3) and they have a
327 higher concentration in the surface samples (24 g kg^{-1} and 445 mg kg^{-1}) than in the
328 subsurface samples (11 g kg^{-1} and 300 mg kg^{-1}). The mean concentration of TOC and P
329 found in the sediment (22 g kg^{-1} and 468 mg kg^{-1}) was close to that observed in the
330 surface sources. K had no correlation with P and TOC, besides having higher
331 concentrations in the surface sources (875 mg kg^{-1}). The K concentration in the
332 sediments varied widely, with a standard deviation closer to the mean (397 ± 362 mg
333 kg^{-1}), which makes this value similar to that found in subsurface sources (565 mg kg^{-1}).
334 Potassium and P presented higher concentrations in the cropland samples due to the
335 addition of fertilizers for crop production. TOC presents higher concentrations in the
336 pastures, which can be attributed to the permanent soil cover and the increase of
337 below-ground biomass induced by well managed animal grazing (López-Mársico et al.,
338 2015; Schuman et al., 1999; Tornquist et al., 2009). Iron was considered as conservative
339 although it did not provide discrimination between sediment sources. This was
340 somehow expected, since highly weathered soils have a high content of Fe oxides across
341 the entire soil profile, making comparison of surface and subsurface sources very

342 difficult. Beryllium was conservative, but its variation between sources was very low,
343 presenting low potential for discrimination between sources (KW *H* test $p > 0.01$).
344 Finally, the LDA selected only P, K and TOC as tracers for the GEO approach, which did
345 not comply with the universal rule of the discriminant analysis for multiple groups,
346 stating that the number of tracers must be at least equivalent to the number of groups
347 (*n*) minus one (*n*-1) (Rencher, 2005). For this reason, the use of geochemical tracers
348 alone was not modelled.

349 In the approach using GEO and M parameters (GM), the LDA selected two
350 magnetic parameters (χ_{LF}, χ_{HF}) and the three previously selected geochemical
351 elements. The two M parameters were highly correlated (Figure 3) and they remained
352 in the same cluster group of tracers, although they differed completely from the group
353 of the other three geochemical elements (Figure 4). Therefore, the LDA kept the two M
354 parameters, which improved the discrimination of the sources, resulting in 74.3% of
355 SCC. The differences of magnetic susceptibility values between sources for the two
356 magnetic parameters, χ_{LF} and χ_{HF}, are similar, where unpaved roads presented higher
357 values (22 x 10^{-6} and 19 x 10^{-6} m^3 kg^{-1}, respectively), followed by croplands, pastures,
358 gullies and stream banks (Table 4). Sediment samples have magnetic susceptibility
359 values (14 x 10^{-6} and 13 x 10^{-6} m^3 kg^{-1}, respectively) closer to those observed for
360 pastures (15 x 10^{-6} and 14 x 10^{-6} m^3 kg^{-1}, respectively) and stream banks (11 x 10^{-6} and
361 10 x 10^{-6} m^3 kg^{-1}, respectively).

362 The same parameters were selected for the combination of GEO and UV
363 parameters (GUV) and the combination of GEO, UV and M parameters (GMUV). For the
364 UV parameters, a, v*, b, L and L* were selected by the LDA, increasing the SCC to 73.3%,
365 an increase of 4.9% compared to the use of GEO tracers alone. The parameter L and L*
366 are related to the variation between white and black colours, also considered as the

luminosity index from HunterLab and CIELAB, respectively. Stream banks, gullies and unpaved roads, which are subsurface sources (mean of 34 and 41 for L and L*, respectively), had the highest values, which means that they have lighter colours than the surface sources (mean of 32 and 39 for L and L*, respectively). L and L* mean values for sediment samples (31 and 37, respectively) were lower than for all sources and closer to those found in surface sources. More positive values for *a* and *b* means that the colour is more red and yellow, respectively. Subsurface sources tend to be more red and yellow, as *a* and *b* values are higher in this material (13.9 and 13.5, respectively) than in surface sources (11.7 and 12.0, respectively). The mean values for sediments (9.0 and 11.4, respectively) were very close to those of the surface sources. The same behaviour was observed for the parameter v* (21.3 and 23.9 for surface and subsurface sources, respectively), which is the CIELUV colour space model derived parameter equivalent to the *a* from CIELAB.

When UV parameters were used individually, the percentage of SCC was the lowest among all the tested tracer combinations, with 59.4% of SCC. The UV parameters selected in this approach were a, v*, v' and b. Besides the other parameters selected in the other approaches, the parameter v' was selected in the UV approach, which is related to the chromacity coordinates u* and v* from the CIELUV model. When the UV and M parameters were combined, two M parameters were selected, but it did not improve the source classification by the DFA, increasing only by 1% the proportion of SCC. The reclassification of source samples by the LDA using the tracers selected in each approach is illustrated in the bi-plot graphs (Figure 5a, 6a, 7a and 8a).

3.2 Model results for each approach

According to the five approaches modelled (UV, MUV, GUV, GM and GMUV), not including the GEO only model as it had insufficient tracers for the number of sources, pasture had the highest sediment contribution for most approaches, except when geochemical tracers were combined with magnetic tracers, supplying sediment proportions ranging from 24 to 33%. Stream bank and cropland were the second and third sources in increasing order of contribution, with contributions ranging from 26 to 31% and 17 to 23%, respectively. Gullies were the fourth contributing source, with a sediment delivery proportion varying between 16 and 19%. Unpaved roads provided the lowest contribution to the river sediment, ranging from 2.6 to 12.2%. The mean relative contributions of each source did not vary significantly between approaches when the mean contributions for all sediment samples are compared, with the exception of unpaved roads, for which the UV approach led to different results (Table 5).

When sediment samples were separated according to the sampling strategy, significant differences between approaches were observed for cropland and unpaved roads for both sampling strategies (Table 5). Comparing the type of sediment samples, cropland had a higher contribution to TISS samples (16 to 39%) compared to FBS samples (15 to 25%). The contribution of pastures to TISS samples was even higher, ranging from 32 to 40%. Unpaved roads had a larger contribution to FBS samples (~10.5%) and contributed less to the TISS samples (~3.5%). For pasture and stream bank, significant differences between approaches were observed for FBS (19.9 to 33.2%) and TISS (16.8 to 31.8%) samples, respectively, while for gullies no difference was observed for any sampling strategy.

The differences in sediment source contributions are mainly observed between the approaches with only alternative tracers (UV and MUV) to those with geochemical parameters included. Figure 5b to 8b provide box plots demonstrating the variation in mean source contributions for all sediment samples when taking into account the 2500 Monte Carlo interactions results obtained for each approach. The large variations in source contributions obtained for each set of simulations resulted in a standard deviation (SD) that varied between 19 and 34% depending on the source considered (Table 5).

The sediment source contributions predicted by the five approaches were similar for the samples collected following the FBS sampling strategy, while the variation between approaches was higher for the TISS samples (Figure 9). Pasture provided the main source of TISS samples according to all approaches, contributing more than 32% of sediment, followed by cropland with more than 24%, with the exception of the approaches based on UV and MUV parameters, according to which cropland contributed only 16 and 18% of sediment, respectively. For the FBS samples, stream bank provided the main source of sediment, contributing more than 25% of the material delivered to the river, with the exception of the approaches based on UV and MUV parameters, according to which pasture was the main source of sediment, with 33 and 31%, respectively.

4 Discussion

4.1 Tracer selection and discrimination between sources

The conservative behaviour of a sediment property may vary according to different factors (e.g. physical, biochemical and geochemical), requiring an appropriate

438 selection of those that do not suffer modifications from their sources to the sediment
439 sampling site, avoiding uncertainties in the sediment fingerprinting technique (Koiter et
440 al., 2013; Sherriff et al., 2015). There are different strategies to verify that a certain
441 tracer is conservative or not, such as the commonly used range test (Navratil et al.,
442 2012; Palazón and Navas, 2017a; Smith and Blake, 2014), where the value of a given
443 tracer measured in sediment must lie within the range of values observed in the
444 sources. However, the statistical test chosen can select different tracers and,
445 consequently, lead the final mixing model to provide different results (Gaspar et al.,
446 2019). In addition, the conservatism test based on mathematical and statistical tests
447 only cannot confirm that the tracer behaves conservatively (Collins et al., 2017b).
448 In the current research, the classical range test based on the maximum and
449 minimum values found in the source samples indicated that 87% of the total variables
450 were conservative, while with the IQR test, only 30% were considered to be
451 conservative. The range test based on maximum and minimum values observed in the
452 sources is less restrictive because, with this test, having only one extreme value for a
453 source sample is sufficient to make the range wider. At the same time, if only one
454 sediment sample has a value outside of the range, it is sufficient to remove the
455 parameter from further analysis. This situation was observed for K and TOC, which
456 were not retained after applying the minimum/maximum range test, because K was not
457 detected in two sediment samples and TOC had a higher concentration in one sediment
458 sample than in the sources, removing two of the three commonly best geochemical
459 tracers used to discriminate potential sediment sources in agricultural catchments. The
460 range test based on IQR proposed by Batista et al. (2018) provided more reasonable
461 results, as it kept only those tracers for which the values measured in the target samples
462 lied within the range found in the sources. Accordingly, it allowed keeping parameters

463 that would have been removed otherwise because only one sediment sample was
464 outside of the range of values measured in the sources. Future research considering the
465 application of alternative conservativeness tests for this homogeneous catchment, such
466 as bi-plots or more complex methods considering organic carbon and particle size
467 dependency, may help to select the most appropriate tracers (Smith et al., 2018; Lizaga
468 et al., 2020).

469 The potential of multiple sets of tracers to improve the discrimination between
470 potential sources is clearly shown by the LDA biplot analysis. However, in none of the
471 combinations tested, there was a clear distinction between potential source groups.
472 According to the distribution of dots and ellipses, there is an overlap of groups,
473 especially for the approaches UV and MUV. The combination of GEO with the other sets
474 of tracers, M and UV, improved the discrimination between two groups: surface
475 (pasture and cropland) and subsurface sources (stream bank, unpaved road and gully).
476 The lack of clear discrimination evident in the LDA biplots likely adds uncertainty to the
477 model results.

478 The soils of the catchment are naturally poor in K and P, two of the main
479 macronutrients essential for crop growth and productivity. The addition of fertilizers in
480 croplands and pastures explains the higher concentration of these elements in surface
481 sources, which differed significantly from those found in subsurface sources. The TOC
482 concentration in the Ferralsols of the region is usually higher in the upper layer of the
483 soil, due to the addition of carbon by the plant residues and roots, as observed in a study
484 of Bortolon et al. (2011), where soil analyses had a mean concentration 1.5 times higher
485 in the uppermost 10 cm of the soil compared to the 10-20 cm layer. Indeed, these three
486 tracers (P, K and TOC) have great potential for tracing agricultural land uses. However,
487 the three geochemical tracers selected in the current research (P, TOC and K) are

488 usually removed from analysis in most sediment fingerprinting studies, as they are
489 generally considered to be easily enriched or depleted during the erosion process
490 (Palazón and Navas, 2017b; Smith and Blake, 2014). Even though, most studies end up
491 discarding these elements without performing any range tests to assess their
492 conservativeness. For example, in an evaluation of 60 studies that evaluated P as a
493 potential tracer, only 27 of them applied a range test, and of these, P was conservative in
494 85% of cases (Tiecher et al., 2019). Moreover, this parameter was selected to model
495 source contributions in 43% of the 60 sediment fingerprinting studies that were
496 reviewed in Tiecher et al. (2019).

497 The transformation of the sediment composition during the erosion and river
498 transport processes is variable depending on the study site considered. The TOC levels
499 found in sediment samples collected in a previous study conducted in the Conceição
500 River catchment (Tiecher et al., 2018) had a lower concentration in the target material
501 compared to that found in the sources, while in the study of Pulley et al. (2015a)
502 sediment was found to be enriched in TOC compared to potential sources. In
503 catchments with strongly weathered soils rich in iron oxides, P is known to be mainly
504 transported in particulate form in the rivers (Bender et al., 2018). This strong chemical
505 adsorption to soil and sediment particles may preserve the P source signature during
506 their transfer in river systems. The no-tillage farming that is main soil management
507 system in the Conceição catchment in soils with a high content of clay and iron oxides
508 may have induced the physico-chemical protection of C and P into micro aggregates (Six
509 et al., 2002; Snyder and Vázquez, 2005). TOC and P are highly correlated as shown in
510 Figure 3, and the strong physical-chemical protection of these elements may support
511 their conservative behaviour. Furthermore, the conservative behaviour of Fe
512 demonstrates that the reduction from its solid state (oxides with Fe^{3+}) to the aqueous

513 one (Fe^{2+}) is not an important process during sediment transport in this catchment,
514 allowing the conservation of the source characteristics.

515 Soil organic carbon, water content, iron oxides and chemical composition are the
516 main parameters responsible for the soil colour (Ben-dor et al., 1998). Although the TOC
517 content had a low correlation with the colour parameters, this parameter can create a
518 source of error in the colour indices, especially when there is a small colour difference
519 between the potential sources (Pulley and Rowntree, 2016a). The soils of the Conceição
520 River catchment are rich in iron oxides, mainly found as goethite and hematite, and
521 colour parameters are closely linked to their respective content in the soils (Schaefer et
522 al., 2008). The A3 index, which is related to the electron pair transition of hematite, have
523 a strong correlation with most colour parameters (data not presented), highlighting the
524 importance of iron oxides in defining the soils and sediment colours in this catchment.
525 Hematite is responsible for the red colour of Ferralsols, while goethite is responsible for
526 the brownish-reddish yellow colour of soils (Cornell and Schwertmann, 2003). The Hr
527 index, which cannot be used in the mixing model because it is not linearly additive,
528 represents the proportion of hematite in the pool of iron oxides (goethite + hematite).
529 Although the soils in the region are predominantly red in colour, their content in
530 goethite is higher than in hematite (Ramos et al., 2020). The Hr index had lower values
531 in the stream banks compared to the other sources, since there is a greater tendency to
532 form goethite in relief positions characterised by the accumulation of water, where
533 ferrihydrite tends to dissolve and form goethite in its place (Schaefer et al., 2008).

534 Owing to the homogeneity of the soil types due to their intense chemical
535 weathering found in the Conceição catchment, the difference in colour and iron oxide
536 parameters between land uses (pastures and croplands) is very low. Differences
537 between surface and subsurface sources tend to be more evident, since a difference in

538 TOC and clay content is usually observed in this type of soils (Table 4) (Testoni et al.,
539 2017). A similar observation is valid for magnetic parameters, which are closely related
540 to the ferromagnetic properties of the soil, which are in turn mainly controlled by
541 particle size and the nature of parent material (Pulley and Rowntree, 2016b). As the
542 potential sources evaluated are originated from very similar soil types and parent
543 material in our catchment, M and UV parameters did not improve significantly the
544 discrimination between land use-based sources.

545 In the same way as with the GEO parameters selected, UV and M likely provided
546 stronger discrimination between surface and subsurface sources. When UV parameters
547 were used in isolation, they were able to classify correctly almost 60% of the samples in
548 their respective groups, which is not so different from the %SCC obtained with GEO
549 tracers alone (68%), according to the LDA. This demonstrates the potential of UV and M
550 tracers to provide a low-cost alternative to GEO tracers. Although UV parameters were
551 not very effective alone in the current research, they have already been used
552 successfully in other case studies (Evrard et al., 2019; Pulley et al., 2018).

553 The low conservativeness of the tracers tested may also be associated with
554 particle size issues (Laceby et al., 2017). Owing to time and financial constraints it was
555 not possible to conduct particle size analyses. Future studies should also consider
556 assessing how particle size may affect conservativeness during erosion, transport and
557 deposition processes in large river catchments. Furthermore, clay soils with high levels
558 of iron oxides, as observed in the present catchment, often form strong stable
559 microaggregates, during erosion process and transport processes, which may behave
560 similarly to coarse particles (silt and sand) (Droppo et al, 2005). Future research should
561 therefore investigate how microaggregates may also affect tracer conservativeness in
562 sediment fingerprinting research in large scale catchments.

4.2 Mixing model results

The results of the mixing model are impacted by the relatively bad quality of the sediment source discrimination. The small difference in tracer signature observed within a given group (surface or subsurface) introduces high uncertainties in the mixing model (Pulley et al., 2017a). The mixing model results in a large IQR, which means that the uncertainty in the model predictions is high. However, the mean results are similar to those observed by Tiecher et al. (2018), who showed that surface sources provided the main source of suspended sediment collected following the TISS strategy, and subsurface sources, mainly stream bank, supplied the main source for FBS samples. The model results according to the different sets of tracers were consistent and there were no major differences between them. Although there is some correlation between the selected parameters in each approach (Figure 3), the potential effect of this collinearity cannot be tested without artificial mixtures, which should be recommended for future research.

Pasture and cropland were poorly distinguished by the discriminant analysis. As a consequence, the mixing model predicted a larger contribution of pastures, which is not consistent with the situation observed in the catchment, where the percentage of land use occupied by pasture is much lower (maximum of 11.9%) and where soil erosion remains limited under this land use. Unpaved roads provided the source that contributed the least to sediment, as observed by Tiecher et al. (2018). Considering the mean source contributions obtained in the current research, they remained consistent with our overall understanding of the hydro-sedimentary behaviour of the catchment, although the high uncertainties associated with the model predictions limited the potential use that could be made of these calculated contributions (e.g. for catchment and river management). In that, the results of the current research strongly differed

588 from those of Chen et al. (2019), who obtained a good discrimination between land uses
589 using the geochemical composition in a catchment with similar geological conditions in
590 the Three Gorges Dam Region, China. However, this study was conducted in two small
591 catchments (0.78 and 0.46 km^2) with shallow (< 50 cm depth) and poorly developed
592 soils with rock fragments, and land use management was also very different.
593 Accordingly, this shows that considering the homogeneity of geological conditions is not
594 sufficient to derive the tracer list as different pedogenic processes and land use
595 mangement may impact the tracing properties.

596 The selection of tracers to be used in each study is generally defined by the
597 constraints of financial resources and access to the analytical facilities (Collins et al.,
598 2017a). However, the priority should be given to the physico-chemical basis supporting
599 the potential sediment source. UV or M properties are often suggested as low cost
600 tracers, but in a catchment with limited geological variability and intense chemical
601 weathering such as under tropical conditions, their use is not straightforward. Indeed,
602 soils had almost homogeneous chemical compositions and a reddish colour through the
603 whole soil profile. Under these conditions, UV had low variability and does not provide a
604 good tracer for discriminating land use-based sources. The need to add a set of different
605 tracers in sediment fingerprinting studies is expected to increase as geological and soil
606 type variability increases in the catchment, as well as the number of sources of interest
607 increases.

608 As a consequence, the discrimination between the sources achieved in the
609 current research remained low, and the modelling results uncertain. Furthermore, as
610 observed by Haddadchi et al. (2013), mixing models may lead to different results
611 depending on the input data. To avoid this problem, the use of tracers with >90% of SCC
612 or the preparation of artificial mixtures for model validation should be systematically

recommended in future sediment fingerprinting approaches. Indeed, there may simply be limitations to the efficacy of the sediment fingerprinting technique in catchments with homogeneous geology or soil types that can be found in many regions of the world, mainly under tropical climates where soils are highly weathered.

A significant proportion of the most productive soils around the world are found under these conditions, and this situation strengthens the need to develop new approaches to discriminate between these land use-based sources. Alternative tracers such as environmental DNA (Foucher et al., 2020) and compound specific stable isotopes (CSSI) (Blake et al., 2012) may provide a powerful alternative to trace the contribution of specific land use sources to sediment. However, technical solutions allowing for the global application of these methods still need to be developed (Brandt et al., 2018; Evrard et al., 2019). Moreover, the application of these vegetation specific related tracers maybe even more challenging in large tropical catchments, characterised by transient and heterogeneous land uses which are often scarcely documented. Accordingly, their use in combination with more conventional tracers may provide a solution to provide consistent and reliable estimations of sediment source contributions to help achieving sustainable agricultural development goals in these regions.

5 Conclusions

The use of alternative tracers based on ultraviolet-visible spectra combined with geochemical parameters improved the sediment source discrimination in the Conceição River catchment. However, the low differences in source signatures observed in this study site resulted in high uncertainties associated with the model predictions, which is mainly due to the homogeneous soil types occurring in the catchment, which are highly weathered and which have a low variability between land uses, as well as between

surface and subsurface sources. Furthermore, in such a homogeneous catchment, the low differences between sources observed for almost all the tested parameters increased the probability of sediments to lie outside of the range observed in the sources and to be removed by the range/conservative tests, which further reduced the number of tracer options.

Magnetic, geochemical and ultraviolet-visible derived parameters have proven to be relatively ineffective for tracing land use-based sources in the Conceição River catchment. When using only one set of tracers, which does not provide a robust discrimination between the sources leading to low percentages of correctly classified samples by the LDA, the results of the model should be used with caution, since they are associated with large uncertainties. This study presents results that differ from those commonly observed in the literature, where additional tracers generally have positive results, showing that the sediment fingerprinting technique may not provide meaningful results in all situations. Tracers with a greater potential for land use discrimination, such as environmental DNA or CSSI, could provide an alternative for better understanding soil erosion processes in the Conceição River catchment and other similar homogeneous catchments worldwide. As such, future research should investigate the efficacy of these next generation tracers in increasingly difficult tracing environments with more attention to the potential impact of particle size on them.

6 Acknowledgments

The authors would like to thank to Conselho Nacional de Pesquisa - CNPq, Coordenação de Aperfeiçoamento de Pessoal de Nível Superior - CAPES, Financiadora de Estudos e Projetos – FINEP for providing financial support. Furthermore, the authors

661 are grateful to the “Mais Água” and FAPERGS PRONEX n° 008/2009 projects for their
662 support. The authors are also grateful to CAPES for founding the PhD scholarship of the
663 first author Rafael Ramon in the framework of the CAPES-COFECUB Project No.
664 88887.196234/2018-00.
665

666 7 References

667 Almagro, Andre, Almagro, André, Oliveira, P.T.S., Nearing, M.A., Hagemann, S., 2017.
668 Projected climate change impacts in rainfall erosivity over Brazil Projected climate
669 change impacts in rainfall erosivity over Brazil 0–12.
670 https://doi.org/10.1038/s41598-017-08298-y

671 Anache, J.A.A., Wendland, E.C., Oliveira, P.T.S., Flanagan, D.C., Nearing, M.A., 2017. Runoff
672 and soil erosion plot-scale studies under natural rainfall: A meta-analysis of the
673 Brazilian experience. CATENA 152, 29–39.
674 https://doi.org/10.1016/j.catena.2017.01.003

675 Batista, P.V.G., Laceby, J.P., Silva, M.L.N., Tassinari, D., Bispo, D.F.A., Curi, N., Davies, J.,
676 Quinton, J.N., 2018. Using pedological knowledge to improve sediment source
677 apportionment in tropical environments. J. Soils Sediments.
678 https://doi.org/10.1007/s11368-018-2199-5

679 Belmont, P., Willenbring, J.K., Schottler, S.P., Marquard, J., Kumarasamy, K., Hemmis, J.M.,
680 2014. Toward generalizable sediment fingerprinting with tracers that are
681 conservative and nonconservative over sediment routing timescales. J. Soils
682 Sediments 14, 1479–1492. https://doi.org/10.1007/s11368-014-0913-5

683 Ben-dor, E., Irons, J., Epema, G.F., 1998. Soil Reflectance, in: Rencz, A.N. (Ed.), Remote
684 Sensing for the Earth Sciences. Manual of Remote Sensing. John Wiley & Sons, Ltd,

New York, pp. 111–188.

Bender, M.A., dos Santos, D.R., Tiecher, T., Minella, J.P.G., de Barros, C.A.P., Ramon, R., 2018. Phosphorus dynamics during storm events in a subtropical rural catchment in southern Brazil. Agric. Ecosyst. Environ. 261. https://doi.org/10.1016/j.agee.2018.04.004

Blake, W.H., Ficken, K.J., Taylor, P., Russell, M.A., Walling, D.E., 2012. Tracing crop-specific sediment sources in agricultural catchments. Geomorphology 139–140, 322–329. https://doi.org/10.1016/j.geomorph.2011.10.036Boardman, J., Vandaele, K., Evans, R., Foster, I.D.L., 2019. Off-site impacts of soil erosion and runoff: Why connectivity is more important than erosion rates. Soil Use Manag. 35, 245–256. https://doi.org/10.1111/sum.12496

Bortolon, E.S.O., Mielniczuk, J., Tornquist, C.G., Lopes, F., Bergamaschi, H., 2011. Validation of the Century model to estimate the impact of agriculture on soil organic carbon in Southern Brazil. Geoderma 167–168, 156–166. https://doi.org/10.1016/j.geoderma.2011.08.008

Borrelli, P., Robinson, D.A., Fleischer, L.R., Lugato, E., Ballabio, C., Alewell, C., Meusburger, K., Modugno, S., Schütt, B., Ferro, V., Bagarello, V., Oost, K. Van, Montanarella, L., Panagos, P., 2017. An assessment of the global impact of 21st century land use change on soil erosion. Nat. Commun. 8, 2013. https://doi.org/10.1038/s41467-017-02142-7

Brandt, C., Dercon, G., Cadisch, G., Nguyen, L.T., Schuller, P., Linares, C.B., Santana, A.C., Golosov, V., Benmansour, M., Amenzou, N., Xinbao, Z., Rasche, F., 2018. Towards global applicability? Erosion source discrimination across catchments using compound-specific δ13C isotopes. Agric. Ecosyst. Environ. 256, 114–122. https://doi.org/10.1016/j.agee.2018.01.010

Brosinsky, A., Foerster, S., Segl, K., Kaufmann, H., 2014a. Spectral fingerprinting:

711 sediment source discrimination and contribution modelling of artificial mixtures
712 based on VNIR-SWIR spectral properties. J. Soils Sediments 14, 1949–1964.
713 https://doi.org/10.1007/s11368-014-0925-1
714 Brosinsky, A., Foerster, S., Segl, K., López-Tarazón, J.A., Piqué, G., Bronstert, A., 2014b.
715 Spectral fingerprinting: characterizing suspended sediment sources by the use of
716 VNIR-SWIR spectral information. J. Soils Sediments 14, 1965–1981.
717 https://doi.org/10.1007/s11368-014-0927-z
718 Caner, L., Petit, S., Joussein, E., Fritsch, E., Herbillon, A.J., 2011. Accumulation of organo-
719 metallic complexes in laterites and the formation of Aluandic Andosols in the
720 Nilgiri Hills (southern India): similarities and differences with Umbric Podzols. Eur.
721 J. Soil Sci. 62, 754–764. https://doi.org/10.1111/j.1365-2389.2011.01389.x
722 Chen, F., Wang, X., Li, X., Wang, J., Xie, D., Ni, J., Liu, Y., 2019. Using the sediment
723 fingerprinting method to identify the sediment sources in small catchments with
724 similar geological conditions. Agric. Ecosyst. Environ. 286, 106655.
725 https://doi.org/10.1016/j.agee.2019.106655
726 Chen, M., Ma, L.Q., 2001. Comparison of Three Aqua Regia Digestion Methods for Twenty
727 Florida Soils. Soil Sci. Soc. Am. J. 65, 491–499.
728 https://doi.org/10.2136/sssaj2001.652491x
729 CIE, 1978. Commission Internationale d'Eclairage. Recommendations on Uniform
730 Colour Spaces, Colour Difference Equations, Psychometrice Colour Terms. J. Oral
731 Rehabil.
732 CIE, C.I. de l'Eclairage, 1931. Commission Internationale de l'Eclairage (CIE), in: CIE
733 Proceedings. Cambridge University Press, Cambridge, UK.
734 Collins, A.L., Foster, I.D.L., Gellis, A.C., Porto, P., Horowitz, A.J., 2017a. Sediment source
735 fingerprinting for informing catchment management: Methodological approaches,

problems and uncertainty. J. Environ. Manage. 194, 1–3. https://doi.org/10.1016/j.jenvman.2017.03.026

Collins, A.L., Pulley, S., Foster, I.D.L., Gellis, A., Porto, P., Horowitz, A.J., 2017b. Sediment source fingerprinting as an aid to catchment management: A review of the current state of knowledge and a methodological decision-tree for end-users. J. Environ. Manage. 194, 86–108. https://doi.org/10.1016/j.jenvman.2016.09.075

Collins, A.L., Walling, D.E., Webb, L., King, P., 2010a. Apportioning catchment scale sediment sources using a modified composite fingerprinting technique incorporating property weightings and prior information. Geoderma 155, 249–261. https://doi.org/10.1016/j.geoderma.2009.12.008

Collins, A.L., Zhang, Y., Walling, D.E., 2010b. Apportioning sediment sources in a grassland dominated agricultural catchment in the UK using a new tracing framework. Sediment Dyn. a Chang. Futur. 337, 68–75.

Cornell, R.M., Schwertmann, U., 2003. The iron oxides. Structure, properties, reactions, occurences and uses, Second. ed. WILEY-VCH Verlag GmbH & Co. KGaA, Weinheim.

Da Silva, Y.J.A.B., Do Nascimento, C.W.A., Biondi, C.M., 2014. Comparison of USEPA digestion methods to heavy metals in soil samples. Environ. Monit. Assess. 186, 47–53. https://doi.org/10.1007/s10661-013-3354-5

Didoné, E.J., Gomes Minella, J.P., Andres Schneider, F.J., Londero, A.L., Lefèvre, I., Evrard, O., 2019. Quantifying the impact of no-tillage on soil redistribution in a cultivated catchment of Southern Brazil (1964–2016) with 137Cs inventory measurements. Agric. Ecosyst. Environ. 284, 106588. https://doi.org/10.1016/j.agee.2019.106588

Didoné, E.J., Minella, J.P.G., Merten, G.H., 2015. Quantifying soil erosion and sediment yield in a catchment in southern Brazil and implications for land conservation. J. Soils Sediments 15, 2334–2346. https://doi.org/10.1007/s11368-015-1160-0

Droppo, I.G., Nackaerts, K., Walling, D.E., Williams, N., 2005. Can flocs and water stable

762 soil aggregates be differentiated within fluvial systems? CATENA 60, 1–18.
763 https://doi.org/10.1016/j.catena.2004.11.002
764 EPA, U.S., 2007. “Method 3051A (SW-846): Microwave Assisted Acid Digestion of
765 Sediments, Sludges, and Oils,” Revision 1. Washington, D.C.
766 Evrard, O., Durand, R., Foucher, A., Tiecher, T., Sellier, V., Onda, Y., Lefèvre, I., Cerdan, O.,
767 Laceby, J.P., 2019. Using spectrocolourimetry to trace sediment source dynamics in
768 coastal catchments draining the main Fukushima radioactive pollution plume
769 (2011–2017). J. Soils Sediments. https://doi.org/10.1007/s11368-019-02302-w
770 Evrard, O., Laceby, J.P., Ficetola, G.F., Gielly, L., Huon, S., Lefèvre, I., Onda, Y., Poulenard, J.,
771 2019. Environmental DNA provides information on sediment sources: A study in
772 catchments affected by Fukushima radioactive fallout. Sci. Total Environ. 665, 873–
773 881. https://doi.org/10.1016/j.scitotenv.2019.02.191
774 FAO, 2019. Soil erosion: the gratest challenge for sustainable soil management. Licence:
775 CC BY-NC-SA 3.0 IGO, Rome.
776 Foucher, A., Evrard, O., Ficetola, G.F., Gielly, L., Poulain, J., Giguet-Covex, C., Laceby, J.P.,
777 Salvador-Blanes, S., Cerdan, O., Poulenard, J., 2020. Persistence of environmental
778 DNA in cultivated soils: implication of this memory effect for reconstructing the
779 dynamics of land use and cover changes. Sci. Rep. 10, 1–12.
780 https://doi.org/10.1038/s41598-020-67452-1
781
782 Fritsch, E., Morin, G., Bedidi, A., Bonnin, D., Balan, E., Caquineau, S., Calas, G., 2005.
783 Transformation of haematite and Al-poor goethite to Al-rich goethite and
784 associated yellowing in a ferralitic clay soil profile of the middle Amazon Basin
785 (Manaus, Brazil). Eur. J. Soil Sci. 56, 575–588. https://doi.org/10.1111/j.1365-
786 2389.2005.00693.x
787 Gaspar, L., Blake, W.H., Smith, H.G., Lizaga, I., Navas, A., 2019. Testing the sensitivity of a

multivariate mixing model using geochemical fingerprints with artificial mixtures. Geoderma 337, 498–510. https://doi.org/10.1016/j.geoderma.2018.10.005

Guzmán, G., Quinton, J.N., Nearing, M.A., Mabit, L., Gómez, J.A., 2013. Sediment tracers in water erosion studies: Current approaches and challenges. J. Soils Sediments 13, 816–833. https://doi.org/10.1007/s11368-013-0659-5

Haddadchi, A., Ryder, D.S., Evrard, O., OLLEY, J., 2013. Sediment fingerprinting in fluvial systems: review of tracers, sediment sources and mixing models. Int. J. Sediment Res. 28, 560–578. https://doi.org/10.1016/S1001-6279(14)60013-5

Hatfield, J.L., Sauer, T.J., Cruse, R.M., 2017. Soil : The Forgotten Piece of the Water , Food , Energy Nexus, 1st ed, Advances in Agronomy. Elsevier Inc. https://doi.org/10.1016/bs.agron.2017.02.001

HunterLab, 2015. The basics of color perception and measurement [WWW Document]. URL https://www.hunterlab.com/basics-of-color-theory.pdf?r=false (accessed 7.9.19).

Jia, L., Zhao, W., Zhai, R., Liu, Y., Kang, M., Zhang, X., 2019. Regional differences in the soil and water conservation efficiency of conservation tillage in China. Catena 175, 18–26. https://doi.org/10.1016/j.catena.2018.12.012

Koiter, A.J., Owens, P.N., Petticrew, E.L., Lobb, D.A., 2013. The behavioural characteristics of sediment properties and their implications for sediment fingerprinting as an approach for identifying sediment sources in river basins. Earth-Science Rev. 125, 24–42. https://doi.org/10.1016/j.earscirev.2013.05.009

Kosmas, C.S., Curi, N., Bryant, R.B., Franzmeier, D.P., 1984. Characterization of iron oxide minerals by second-derivative visible spectroscopy. Soil Sci. Soc. Am. J. 48, 401–405. https://doi.org/10.2136/sssaj1984.03615995004800020036x

Laceby, J.P., Evrard, O., Smith, H.G., Blake, W.H., Olley, J.M., Minella, J.P.G., Owens, P.N.,

2017. The challenges and opportunities of addressing particle size effects in sediment source fingerprinting: A review. Earth-Science Rev. 169, 85–103. https://doi.org/10.1016/j.earscirev.2017.04.009

Lal, R., 2007. Anthropogenic Influences on World Soils and Implications to Global Food Security. Adv. Agron. 93, 69–93. https://doi.org/10.1016/S0065-2113(06)93002-8

Legout, C., Poulenard, J., Nemery, J., Navratil, O., Grangeon, T., Evrard, O., Esteves, M., 2013. Quantifying suspended sediment sources during runoff events in headwater catchments using spectrocolorimetry. J. Soils Sediments 13, 1478–1492. https://doi.org/10.1007/s11368-013-0728-9

Lizaga, I., Latorre, B., Gaspar, L., Navas, A., 2020. Consensus ranking as a method to identify non-conservative and dissenting tracers in fingerprinting studies. Sci. Total Environ. 720, 137537. https://doi.org/10.1016/j.scitotenv.2020.137537

López-Mársico, L., Altesor, A., Oyarzabal, M., Baldassini, P., Paruelo, J.M., 2015. Grazing increases below-ground biomass and net primary production in a temperate grassland. Plant Soil 392, 155–162. https://doi.org/10.1007/s11104-015-2452-2

Martínez-Carreras, N., Krein, A., Gallart, F., Iffly, J.F., Pfister, L., Hoffmann, L., Owens, P.N., 2010a. Assessment of different colour parameters for discriminating potential suspended sediment sources and provenance: A multi-scale study in Luxembourg. Geomorphology 118, 118–129. https://doi.org/10.1016/j.geomorph.2009.12.013

Martínez-Carreras, N., Udelhoven, T., Krein, A., Gallart, F., Iffly, J.F., Ziebel, J., Hoffmann, L., Pfister, L., Walling, D.E., 2010b. The use of sediment colour measured by diffuse reflectance spectrometry to determine sediment sources: Application to the Attert River catchment (Luxembourg). J. Hydrol. 382, 49–63. https://doi.org/10.1016/j.jhydrol.2009.12.017

Melo, D.C.D., Anache, J.A.A., Almeida, C. das N., Coutinho, J. V., Ramos Filho, G.M., Rosalem, L.M.P., Pelinson, N.S., Ferreira, G.L.R.A., Schwamback, D., Calixto, K.G.,

839 Siqueira, J.P.G., Duarte-Carvajalino, J.C., Jhunior, H.C.S., Nóbrega, J.D., Morita, A.K.M.,
840 Leite, C.M.C., Guedes, A.C.E., Coelho, V.H.R., Wendland, E., 2020. The big picture of
841 field hydrology studies in Brazil. Hydrol. Sci. J. 0, 1.
842 https://doi.org/10.1080/02626667.2020.1747618
843 Minella, J.P.G., Merten, G.H., Clarke, R.T., 2004. Identification of sediment sources in a
844 small rural drainage basin, in: Sediment Transfer through the Fluvial System
845 (Proceedings of a Symposium Held in Moscow, August 2004). IAHS Press, Moscow,
846 pp. 44–51.
847 Mullins, C.E., 1977. Magnetic Susceptibility of the Soil and Its Significance in Soil Science
848 – a Review. J. Soil Sci. 28, 223–246. https://doi.org/10.1111/j.1365-
849 2389.1977.tb02232.x
850 Navratil, O., Evrard, O., Esteves, M., Legout, C., Ayrault, S., Némery, J., Mate-Marin, A.,
851 Ahmadi, M., Lefèvre, I., Poirel, A., Bonté, P., 2012. Temporal variability of suspended
852 sediment sources in an alpine catchment combining river/rainfall monitoring and
853 sediment fingerprinting. Earth Surf. Process. Landforms 37, 828–846.
854 https://doi.org/10.1002/esp.3201
855 Niu, B., Zhang, X., Qu, J., Liu, B., Homan, J., Tan, L., An, Z., 2019. Using multiple composite
856 fingerprints to quantify source contributions and uncertainties in an arid region. J.
857 Soils Sediments. https://doi.org/10.1007/s11368-019-02424-1
858 Nosrati, K., Collins, A.L., 2019. Investigating the importance of recreational roads as a
859 sediment source in a mountainous catchment using a fingerprinting procedure
860 with different multivariate statistical techniques and a Bayesian un-mixing model.
861 J. Hydrol. 569, 506–518. https://doi.org/10.1016/j.jhydrol.2018.12.019
862 Palazón, L., Navas, A., 2017a. Variability in source sediment contributions by applying
863 different statistic test for a Pyrenean catchment. J. Environ. Manage. 194, 42–53.
864 https://doi.org/10.1016/j.jenvman.2016.07.058
865 Palazón, L., Navas, A., 2017b. Variability in source sediment contributions by applying

different statistic test for a Pyrenean catchment. J. Environ. Manage. 194, 42–53. https://doi.org/10.1016/j.jenvman.2016.07.058

Phillips, J.M., Russell, M.A., Walling, D.E., 2000. Time-integrated sampling of fluvial suspended sediment: A simple methodology for small catchments. Hydrol. Process. 14, 2589–2602. https://doi.org/10.1002/1099-1085(20001015)14:14<2589::AID-HYP94>3.0.CO;2-D

Pimentel, D., 2006. Soil Erosion: A Food and Environmental Threat. Environ. Dev. Sustain. 8, 119–137. https://doi.org/10.1007/s10668-005-1262-8

Poesen, J., 2017. Soil erosion in the Anthropocene: research needs. Earth Surf. Process. Landforms 84, 64–84. https://doi.org/10.1002/esp.4250

Poulenard, J., Legout, C., Némery, J., Bramorski, J., Navratil, O., Douchin, A., Fanget, B., Perrette, Y., Evrard, O., Esteves, M., 2012. Tracing sediment sources during floods using Diffuse Reflectance Infrared Fourier Transform Spectrometry (DRIFTS): A case study in a highly erosive mountainous catchment (Southern French Alps). J. Hydrol. 414–415, 452–462. https://doi.org/10.1016/j.jhydrol.2011.11.022

Pulley, S., Foster, I., Antunes, P., 2015a. The uncertainties associated with sediment fingerprinting suspended and recently deposited fluvial sediment in the Nene river basin. Geomorphology 228, 303–319. https://doi.org/10.1016/j.geomorph.2014.09.016

Pulley, S., Foster, I., Antunes, P., 2015b. The application of sediment fingerprinting to floodplain and lake sediment cores: assumptions and uncertainties evaluated through case studies in the Nene Basin, UK. J. Soils Sediments 15, 2132–2154. https://doi.org/10.1007/s11368-015-1136-0

Pulley, S., Foster, I., Collins, A.L., 2017a. The impact of catchment source group classification on the accuracy of sediment fingerprinting outputs. J. Environ.

Manage. 194, 16–26. https://doi.org/10.1016/j.jenvman.2016.04.048

Pulley, S., Rowntree, K., 2016a. The use of an ordinary colour scanner to fingerprint sediment sources in the South African Karoo. J. Environ. Manage. 165, 253–262. https://doi.org/10.1016/j.jenvman.2015.09.037

Pulley, S., Rowntree, K., 2016b. Stages in the life of a magnetic grain: Sediment source discrimination, particle size effects and spatial variability in the South African Karoo. Geoderma 271, 134–143. https://doi.org/10.1016/j.geoderma.2016.02.015

Pulley, S., Van Der Waal, B., Collins, A.L., Foster, I.D.L., Rowntree, K., 2017b. Are source groups always appropriate when sediment fingerprinting? The direct comparison of source and sediment samples as a methodological step. River Res. Appl. 33, 1553–1563. https://doi.org/10.1002/rra.3192

Pulley, S., Van der Waal, B., Rowntree, K., Collins, A.L., 2018. Colour as reliable tracer to identify the sources of historically deposited flood bench sediment in the Transkei, South Africa: A comparison with mineral magnetic tracers before and after hydrogen peroxide pre-treatment. CATENA 160, 242–251. https://doi.org/10.1016/j.catena.2017.09.018

R Development Core Team, 2017. R: a language and environment for statistical computing.

Ramon, R., Minella, J.P.G., Merten, G.H., de Barros, C.A.P., Canale, T., 2017. Kinetic energy estimation by rainfall intensity and its usefulness in predicting hydrosedimentological variables in a small rural catchment in southern Brazil. CATENA 148, 176–184. https://doi.org/10.1016/j.catena.2016.07.015

Ramos, P.V., Indaa, A.V., Barrón, V., Siqueira, D.S., Júnior, J., Teixeira, D.D.B., 2020. Color in subtropical brazilian soils as determined with a Munsell chart and by diffuse reflectance spectroscopy. Catena 193, 1–26. https://doi.org/10.1016/j.catena.2020.104609

Rencher, A.C., 2005. A Review Of "Methods of Multivariate Analysis, Second Edition." IIE Trans. 37, 1083–1085. https://doi.org/10.1080/07408170500232784

Rowntree, K.M., van der Waal, B.W., Pulley, S., 2017. Magnetic susceptibility as a simple tracer for fluvial sediment source ascription during storm events. J. Environ. Manage. 194, 54–62. https://doi.org/10.1016/j.jenvman.2016.11.022

Schaefer, C.E.G.R., Fabris, J.D., Ker, J.C., 2008. Minerals in the clay fraction of Brazilian Latosols (Oxisols): a review. Clay Miner. 43, 137–154. https://doi.org/10.1180/claymin.qw2008.043.1.11

Scheinost, A.C., Chavernas, A., Barrón, V., Torrent, J., 1998. Use and limitations of second-derivative diffuse reflectance spectroscopy in the visible to near-infrared range to identify and quantify Fe oxide minerals in soils. Clays Clay Miner. 46, 528–536. https://doi.org/10.1346/CCMN.1998.0460506

Schuman, G.E., Reeder, J.D., Manley, J.T., Hart, R.H., Manley, W.A., 1999. Impact of grazing management on the carbon and nitrogen balance of a mixed-grass rangeland. Ecol. Appl. 9, 65–71. https://doi.org/10.1890/1051-0761(1999)009[0065:IOGMOT]2.0.CO;2

Sherriff, S.C., Franks, S.W., Rowan, J.S., Fenton, O., Ó'hUallacháin, D., 2015. Uncertainty-based assessment of tracer selection, tracer non-conservativeness and multiple solutions in sediment fingerprinting using synthetic and field data. J. Soils Sediments 15, 2101–2116. https://doi.org/10.1007/s11368-015-1123-5

Six, J., Feller, C., Denef, K., Ogle, S.M., de Moraes, J.C., Albrecht, A., 2002. Soil organic matter, biota and aggregation in temperate and tropical soils - Effects of no-tillage. Agronomie 22, 755–775. https://doi.org/10.1051/agro:2002043

Smith, H.G., Blake, W.H., 2014. Sediment fingerprinting in agricultural catchments: A critical re-examination of source discrimination and data corrections.

942 Geomorphology 204, 177–191. https://doi.org/10.1016/j.geomorph.2013.08.003
943 Smith, H.G., Evrard, O., Blake, W.H., Owens, P.N., 2015. Preface—Addressing challenges
944 to advance sediment fingerprinting research. J. Soils Sediments 15, 2033–2037.
945 https://doi.org/10.1007/s11368-015-1231-2
946 Smith, H.G., Karam, D.S., Lennard, A.T., 2018. Evaluating tracer selection for catchment
947 sediment fingerprinting. J. Soils Sediments 18, 3005–3019.
948 https://doi.org/10.1007/s11368-018-1990-7
949 Snyder, V.A., Vázquez, M.A., 2005. STRUCTURE, in: Encyclopedia of Soils in the
950 Environment. Elsevier, pp. 54–68. https://doi.org/10.1016/B0-12-348530-
951 4/00533-6
952 Testoni, S.A., de Almeida, J.A., da Silva, L., Andrade, G.R.P., 2017. Clay mineralogy of
953 Brazilian oxisols with shrinkage properties. Rev. Bras. Cienc. do Solo 41, 1–16.
954 https://doi.org/10.1590/18069657rbcs20160487
955 Tiecher, T., Caner, L., Minella, J.P.G., Evrard, O., Mondamert, L., Labanowski, J.,
956 Rheinheimer, D. dos S., 2017. Tracing Sediment Sources Using Mid-infrared
957 Spectroscopy in Arvorezinha Catchment, Southern Brazil. L. Degrad. Dev. 28, 1603–
958 1614. https://doi.org/10.1002/ldr.2690
959 Tiecher, T., Caner, L., Minella, J.P.G., Santos, D.R. dos, 2015. Combining visible-based-
960 color parameters and geochemical tracers to improve sediment source
961 discrimination and apportionment. Sci. Total Environ. 527–528, 135–149.
962 https://doi.org/10.1016/j.scitotenv.2015.04.103
963 Tiecher, T., Minella, J.P.G., Evrard, O., Caner, L., Merten, G.H., Capoane, V., Didoné, E.J., dos
964 Santos, D.R., 2018. Fingerprinting sediment sources in a large agricultural
965 catchment under no-tillage in Southern Brazil (Conceição River). L. Degrad. Dev. 29,
966 939–951. https://doi.org/10.1002/ldr.2917
967 Tiecher, T., Ramon, R., Laceby, J.P., Evrard, O., Minella, J.P.G., 2019. Potential of

968 phosphorus fractions to trace sediment sources in a rural catchment of Southern
969 Brazil: Comparison with the conventional approach based on elemental
970 geochemistry. Geoderma 337, 1067–1076.
971 https://doi.org/10.1016/j.geoderma.2018.11.011
972 Tornquist, C.G., Mielniczuk, J., Cerri, C.E.P., 2009. Modeling soil organic carbon dynamics
973 in Oxisols of Ibirubá (Brazil) with the Century Model. Soil Tillage Res. 105, 33–43.
974 https://doi.org/10.1016/j.still.2009.05.005
975 Torres Astorga, R., de los Santos Villalobos, S., Velasco, H., Domínguez-Quintero, O.,
976 Pereira Cardoso, R., Meigikos dos Anjos, R., Diawara, Y., Dercon, G., Mabit, L., 2018.
977 Exploring innovative techniques for identifying geochemical elements as
978 fingerprints of sediment sources in an agricultural catchment of Argentina affected
979 by soil erosion. Environ. Sci. Pollut. Res. 25, 20868–20879.
980 https://doi.org/10.1007/s11356-018-2154-4
981 Uber, M., Legout, C., Nord, G., Crouzet, C., Demory, F., Poulenard, J., 2019. Comparing
982 alternative tracing measurements and mixing models to fingerprint suspended
983 sediment sources in a mesoscale Mediterranean catchment.
984 van der Waal, B., Rowntree, K., Pulley, S., 2015. Flood bench chronology and sediment
985 source tracing in the upper Thina catchment, South Africa: the role of transformed
986 landscape connectivity. J. Soils Sediments 15, 2398–2411.
987 https://doi.org/10.1007/s11368-015-1185-4
988 Viscarra Rossel, R.A., Minasny, B., Roudier, P., McBratney, A.B.B., 2006. Colour space
989 models for soil science. Geoderma 133, 320–337.
990 https://doi.org/10.1016/j.geoderma.2005.07.017
991 Walkley, A., Black, I.A., 1934. An examination of the Degtjareff Method for determining
992 soil organic matter, and a proposed modification of the chromic acid titration
993 method. Soil Sci. 37, 29–38. https://doi.org/10.1097/00010694-193401000-

994 00003
995 Walling, D.E., 2013. The evolution of sediment source fingerprinting investigations in
996 fluvial systems. J. Soils Sediments 13, 1658–1675.
997 https://doi.org/10.1007/s11368-013-0767-2
998 Walling, D.E., Peart, M.R., Oldfield, F., Thompson, R., 1979. Suspended sediment sources
999 identified by magnetic measurements. Nature 281, 110–113. https://doi.org/0028-
1000 0836/79/370110-04$01.00
1001 Yu, L., Oldfield, F., 1989. A multivariate mixing model for identifying sediment source
1002 from magnetic measurements. Quat. Res. 32, 168–181.
1003 https://doi.org/10.1016/0033-5894(89)90073-2
1004

8 Appendices

8.1 Appendix A

The water discharge (Q) and suspended sediment concentration (SSC) was monitored at the catchment outlet using automatic equipment's that recorded the water level and turbidity every 10 min through a pressure water level sensor and a turbidimeter (Hydrological monitoring station Model SL-2000, Solar®, Brazil), respectively. The Q was calculated from the water level data using a rating curve. The turbidity sensor was properly calibrated with SSC measured data obtained from samples of the water and sediment mixture collected during rainfall-runoff events and in a daily based schedule used for determination of SSC in the laboratory. In the Figure A1 shows the Q and SCC data measured with the automatic equipment's are presented. The period covered by each time integrated sediment samples (TISS) and the date that fine bed sediment samples (FBS) were collected (Table 1) are illustrated in the Figure A1. The first TISS (S-9) was installed after the harvesting of the summer crop season of 2011/2012, and the sample collected before to start the following summer crop season, having a sample which represents the winter period which had less intense rainfall. The second TISS sample (S-10), represents the period in which the soil is more susceptible to erosion processes due to the soil preparation and sowing process, which occurs together with the period of heavier rainfall (September to November). The third sampling period (S-11) represents the period in which the summer crops are stablished and the soil is more protected by the summer crops.

8.2 Appendix B

Twenty-four colour parameters were calculated from the ultraviolet-visible spectra following the colorimetric models described in detail by Viscarra Rossel et al.

(2006), which are based on the Munsell HVC, RGB, the decorrelation of RGB data, CIELAB and CIELUV Cartesian coordinate systems, three parameters from the HuterLab colour space model and two indices (coloration – CI and saturation index – SI). First, the colour coefficients XYZ based on the colour-matching functions defined by the International Commission on Illumination - CIE (CIE, 1931) were calculated, where X and Z are the virtual components of the primary spectra and Y represents the brightness. The XYZ tristimulus were standardised with values corresponding to the Standard Illuminant D65 white point for 10 Degree Standard Observer (X = 94.8110; Y = 100.00; Z = 107.304), then transformed into the Munsel HVC, RGB, CIELAB and CIELUV Cartesian coordinate systems using the equations from CIE (1978). Three parameters from the HunterLab (HunterLab, 2015) colour space model, and two indices (coloration - CI and saturation index - SI) (Pulley et al., 2018) were calculated as well. In total, 27 colour metric parameters were derived from the spectra of potential source and sediment samples (L, L*, a, a*, b, b*, C*, h, RI, x, y, z, u*, v*, u', v', Hvc, hVc, hvC, R, G, B, HRGB, IRGB, SRGB, CI and SI).

Three other parameters were calculated from the second derivative curves of remission functions in the visible range of soil and sediment samples, which displayed three major absorption bands at short wavelengths commonly attributed to Fe-oxides (Caner et al., 2011; Fritsch et al., 2005; Kosmas et al., 1984; Scheinost et al., 1998). The first band (A1, ~430 nm) corresponds to the single electron transition of goethite (Gt), whereas the two others correspond to the electron pair transition for goethite (A2, ~480 nm) and for hematite (Hm) (A3, ~520 nm), respectively (Figure B1). The band intensity is estimated from the amplitude between a minimum and the nearby maximum at its lower energy side. The amplitudes of the three bands (A1, A2 and A3) are positively correlated with the contents of Gt and Hm (Fritsch et al., 2005). A1 and A3

1054 are commonly used to assess the content of Gt and Hm, respectively, and the relative
1055 proportions of hematite in Fe oxides (Hr) are estimated by applying the equation Hr
1056 (%) = Hm/(Hm+Gt). The band intensities were measured from the amplitude between
1057 each band minimum and its nearby maximum at higher wavelength.
1058

Figure 1

Click here to download high resolution image

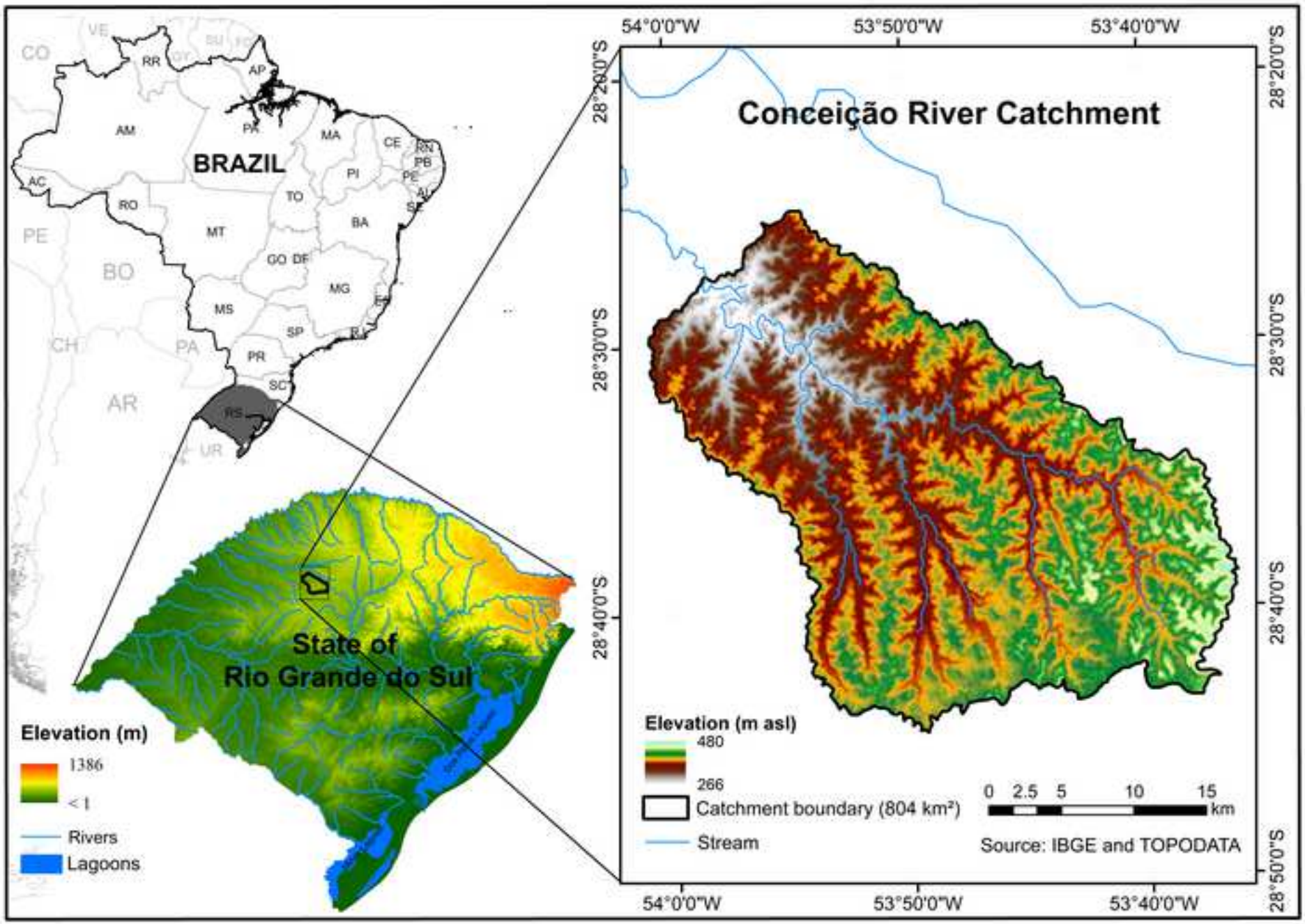

Figure 2

Click here to download high resolution image

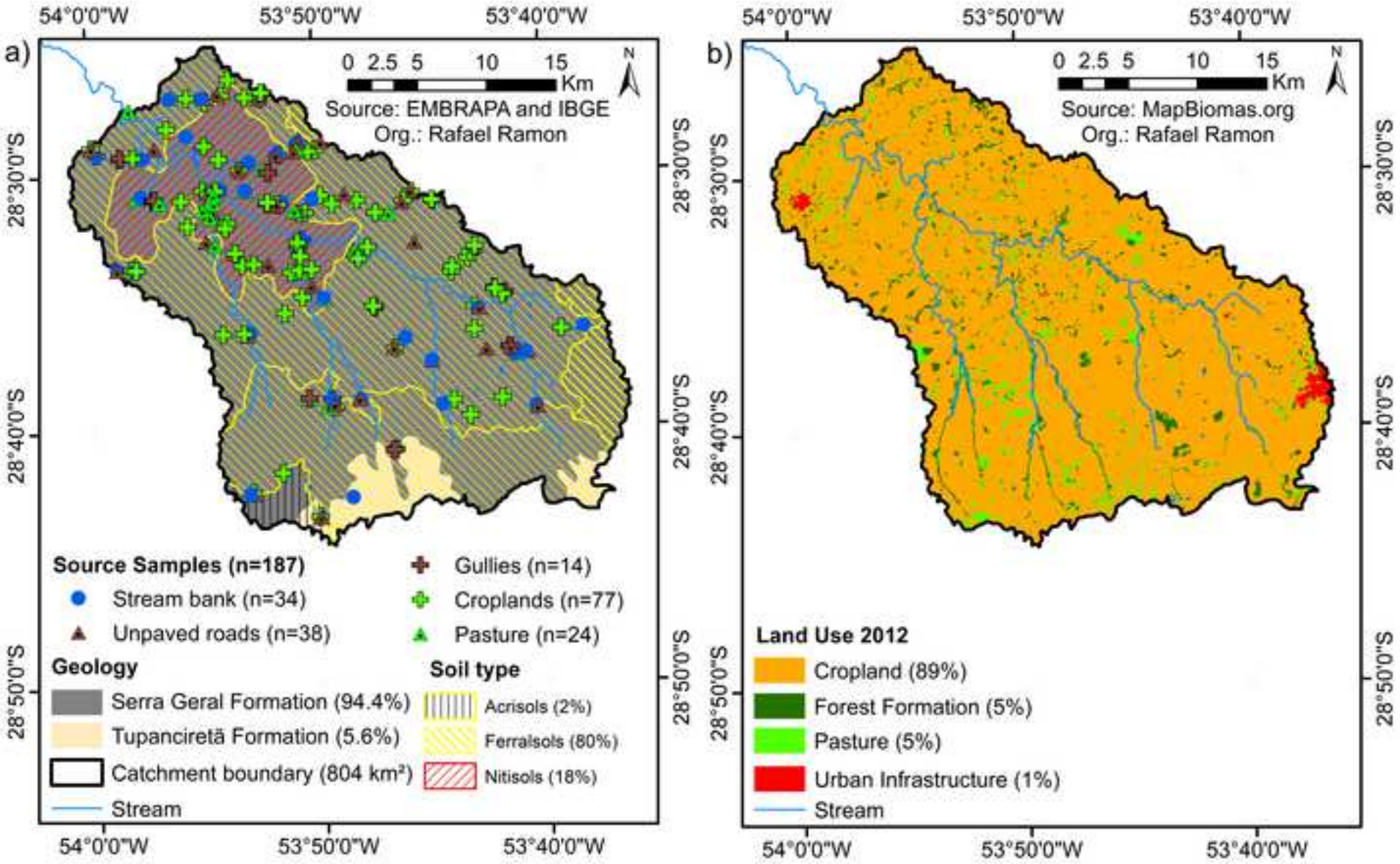

Figure 3

Click here to download high resolution image

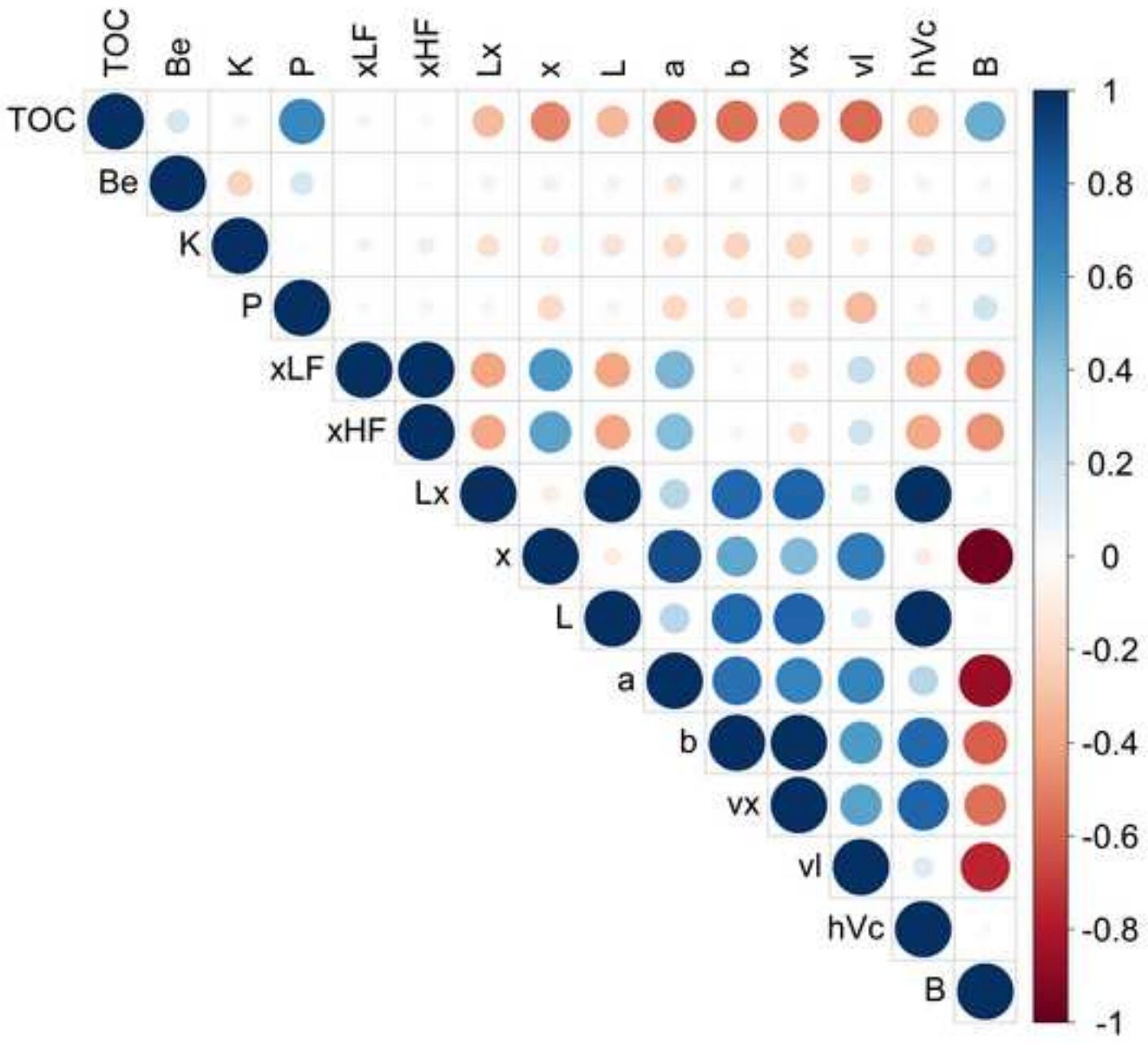

Figure 4

Click here to download high resolution image

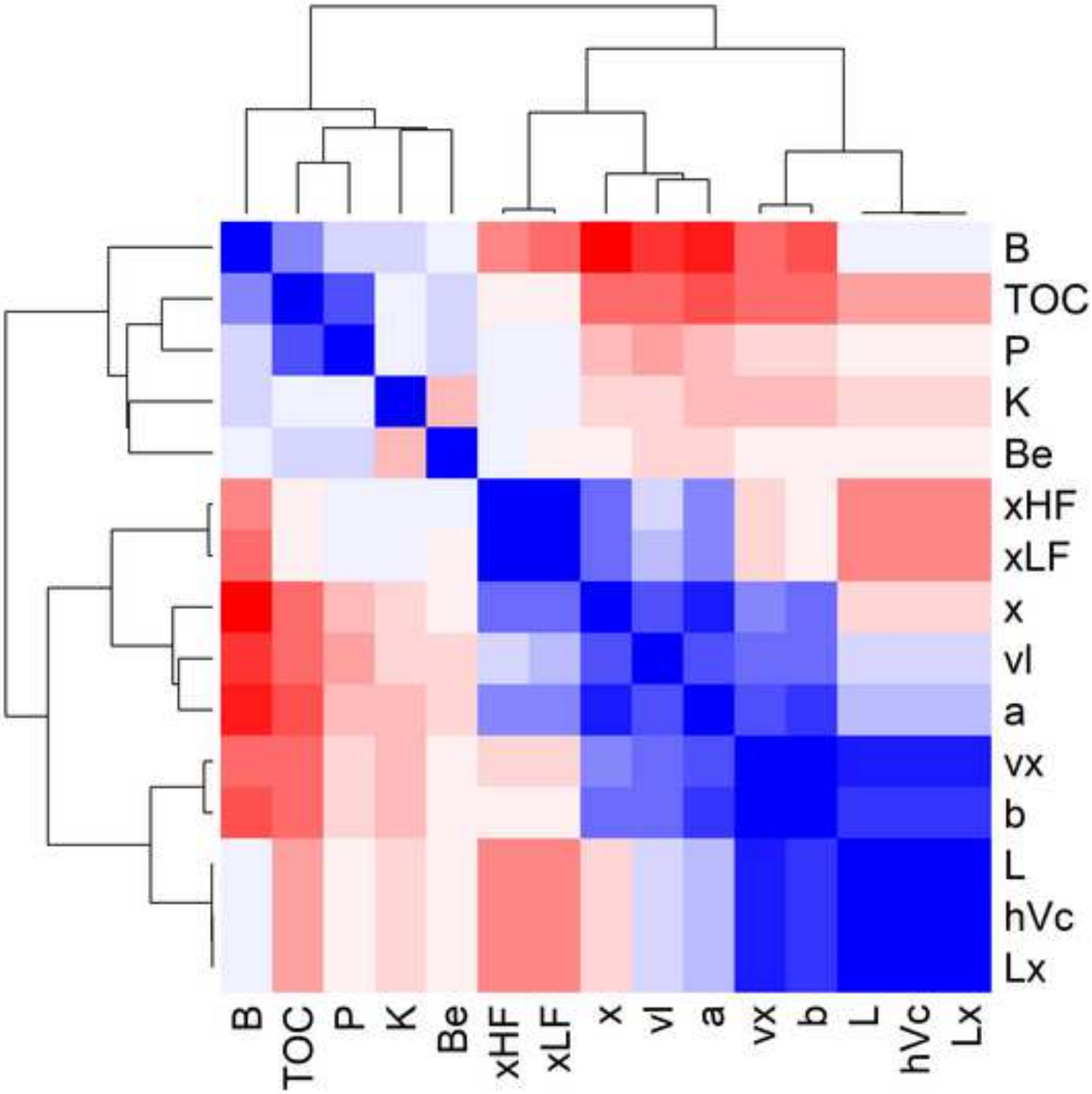

Figure 5

Click here to download high resolution image

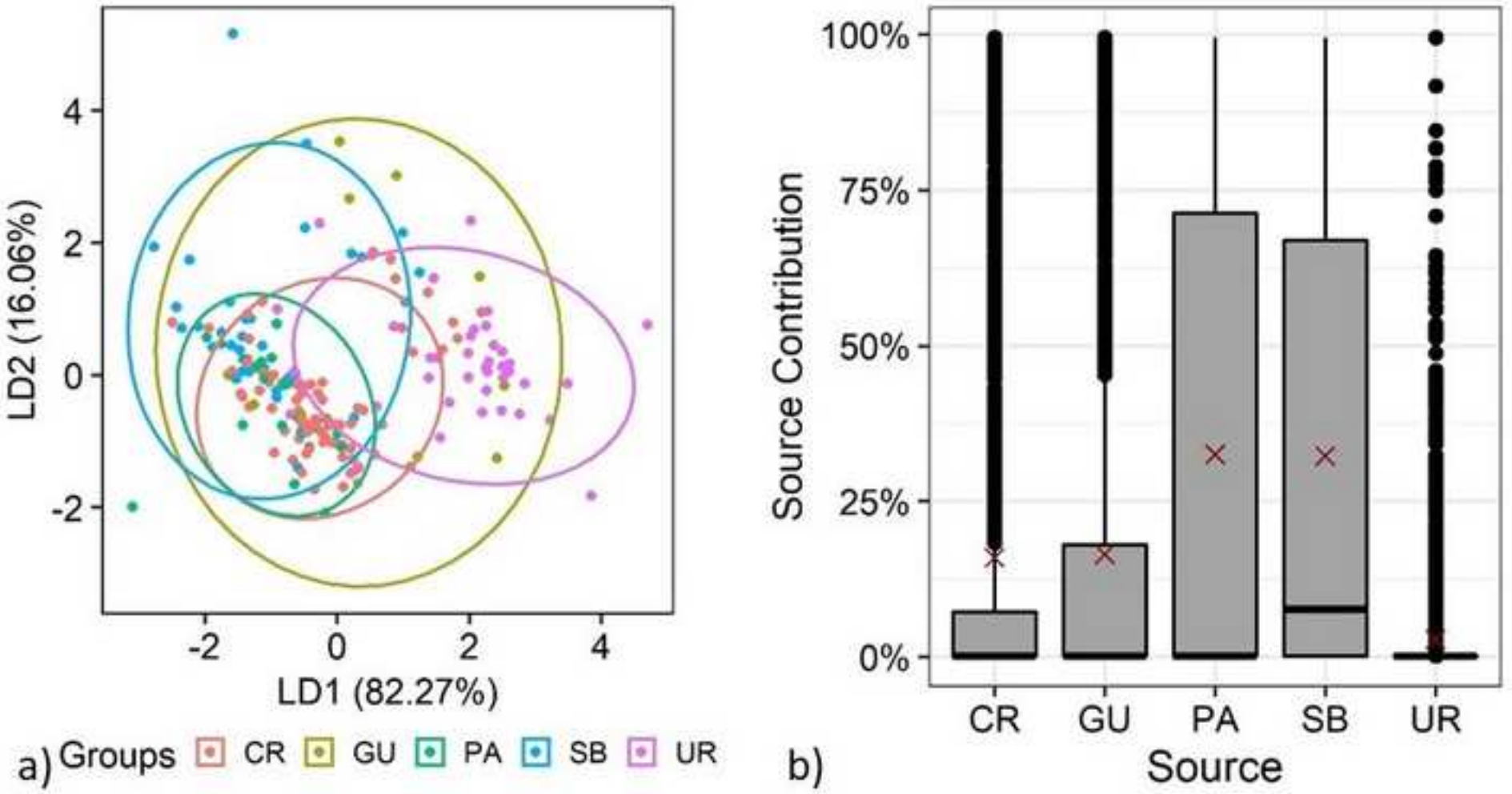

Figure 6

Click here to download high resolution image

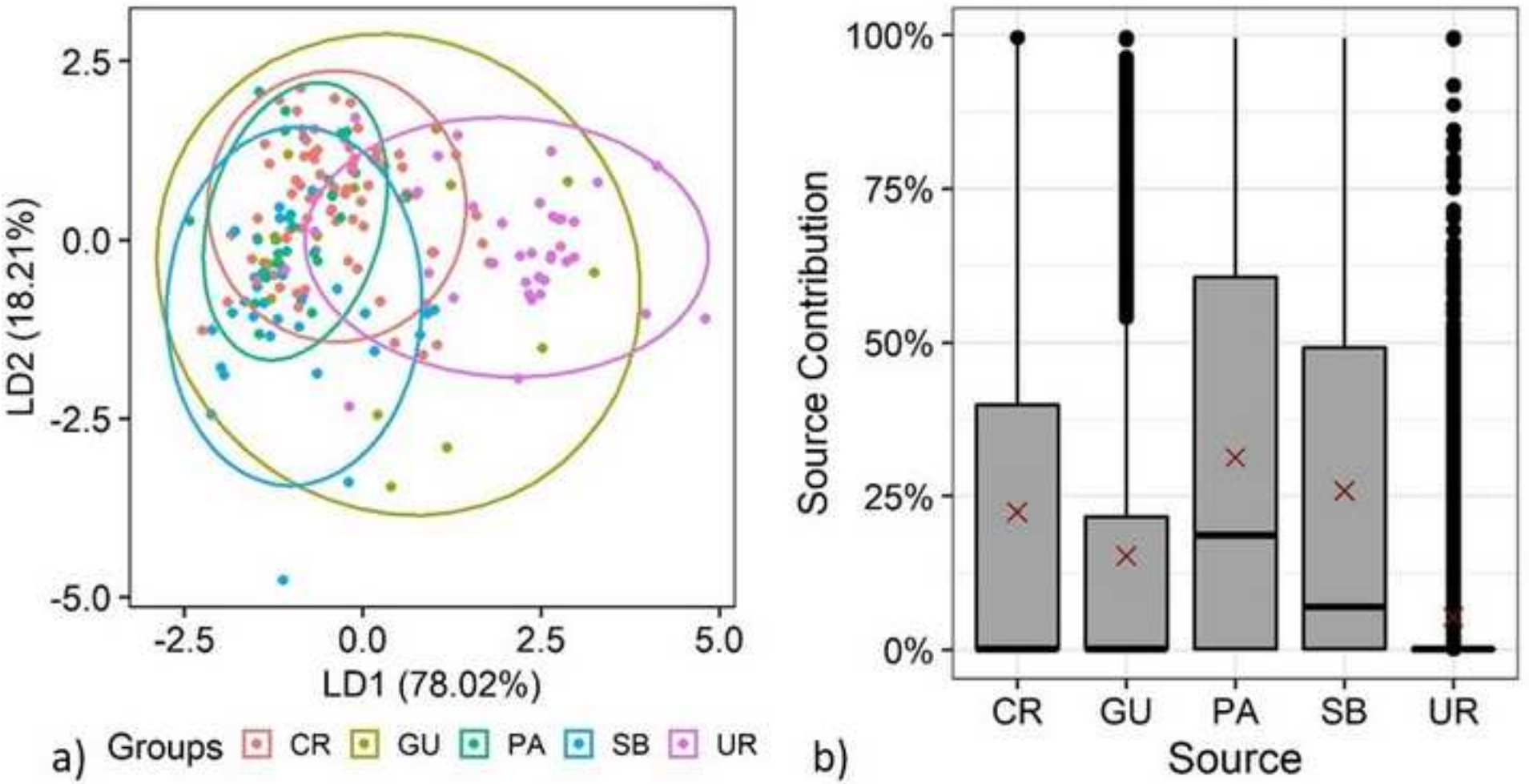

Figure 7

Click here to download high resolution image

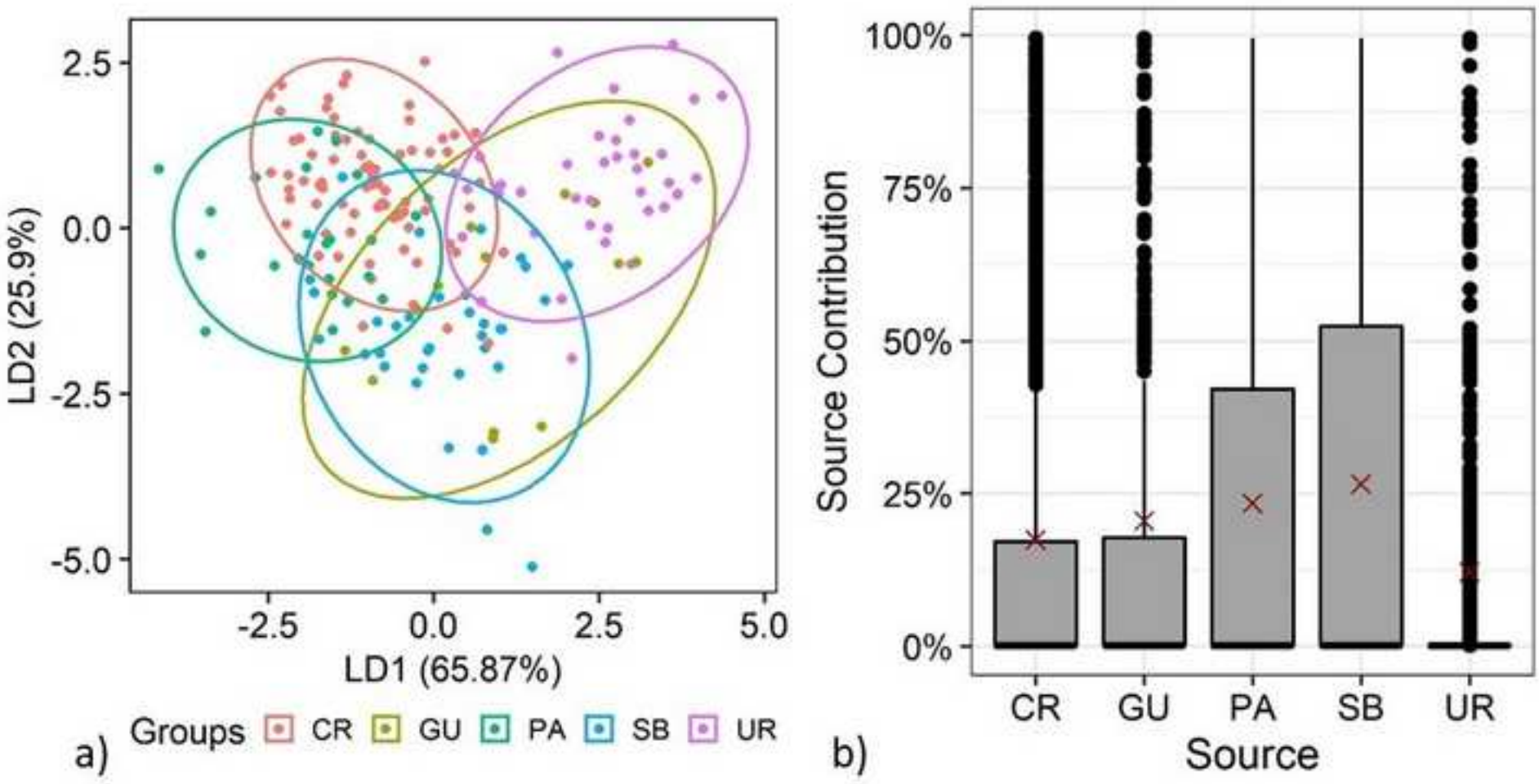

Figure 8

Click here to download high resolution image

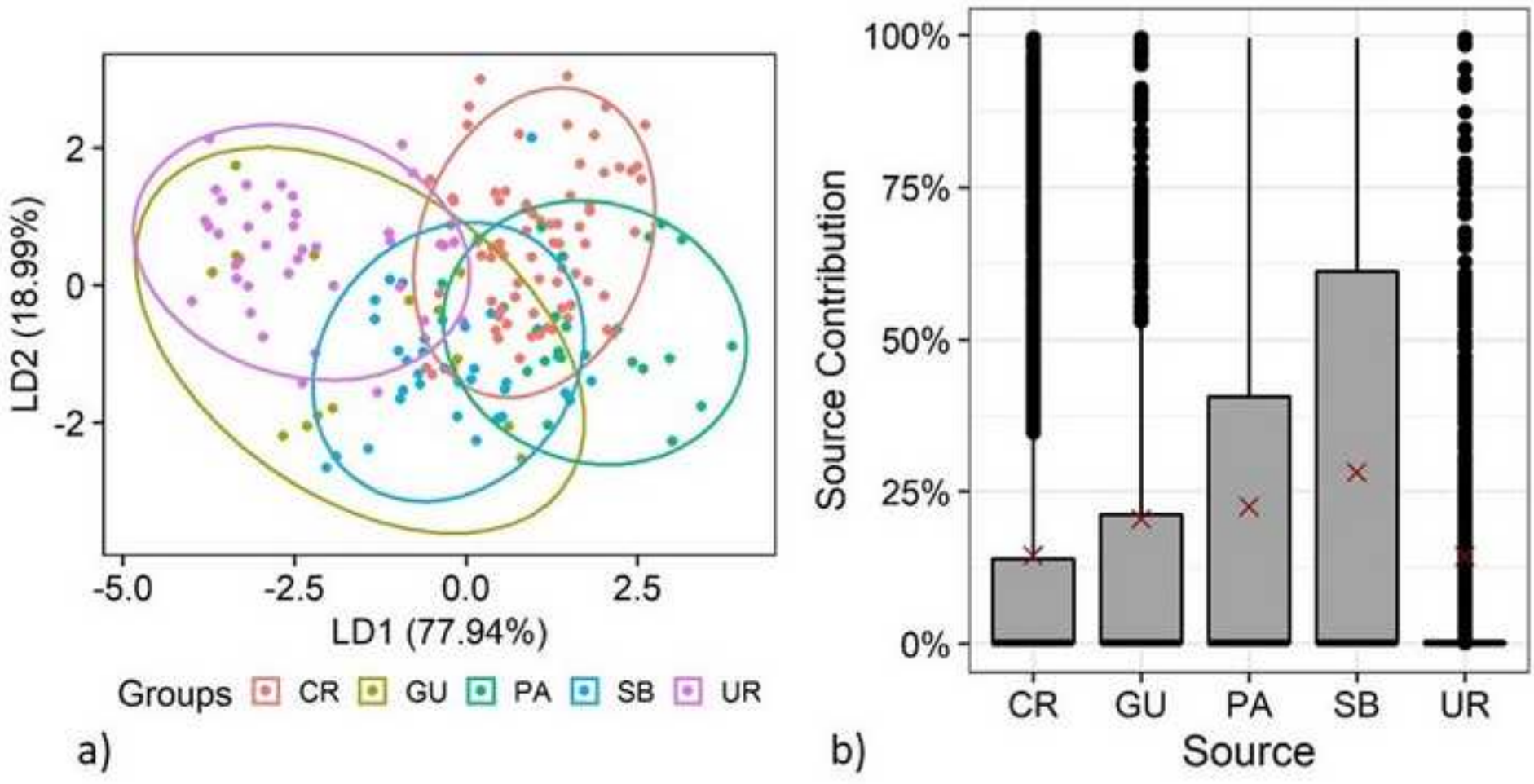

Figure 9

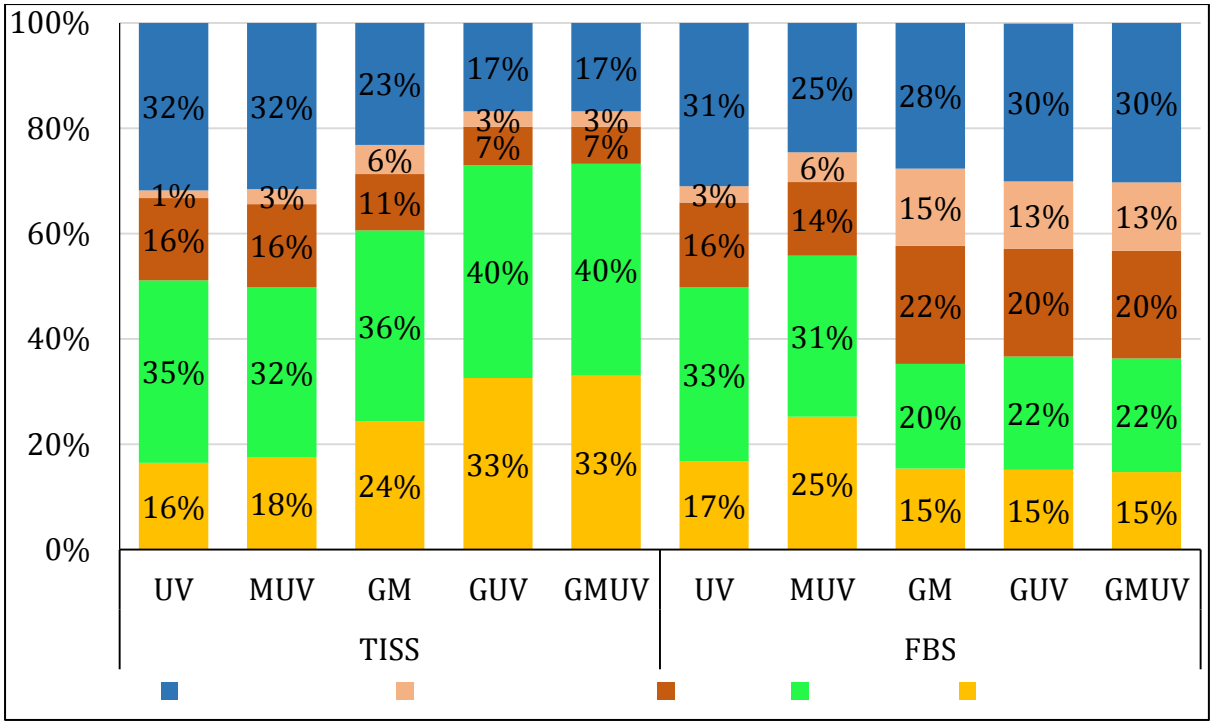
100%
80%
60%
40%
20%
0%
32%
1%
16%
35%
16%
32%
3%
16%
32%
18%
23%
6%
11%
36%
24%
17%
3%
7%
40%
33%
17%
3%
7%
40%
33%
31%
3%
16%
33%
17%
25%
6%
14%
31%
25%
28%
15%
22%
20%
15%
30%
13%
20%
22%
15%
30%
13%
20%
22%
15%
UV
MUV
GM
GUV
GMUV
UV
MUV
GM
GUV
GMUV
TISS
FBS

Figure A1

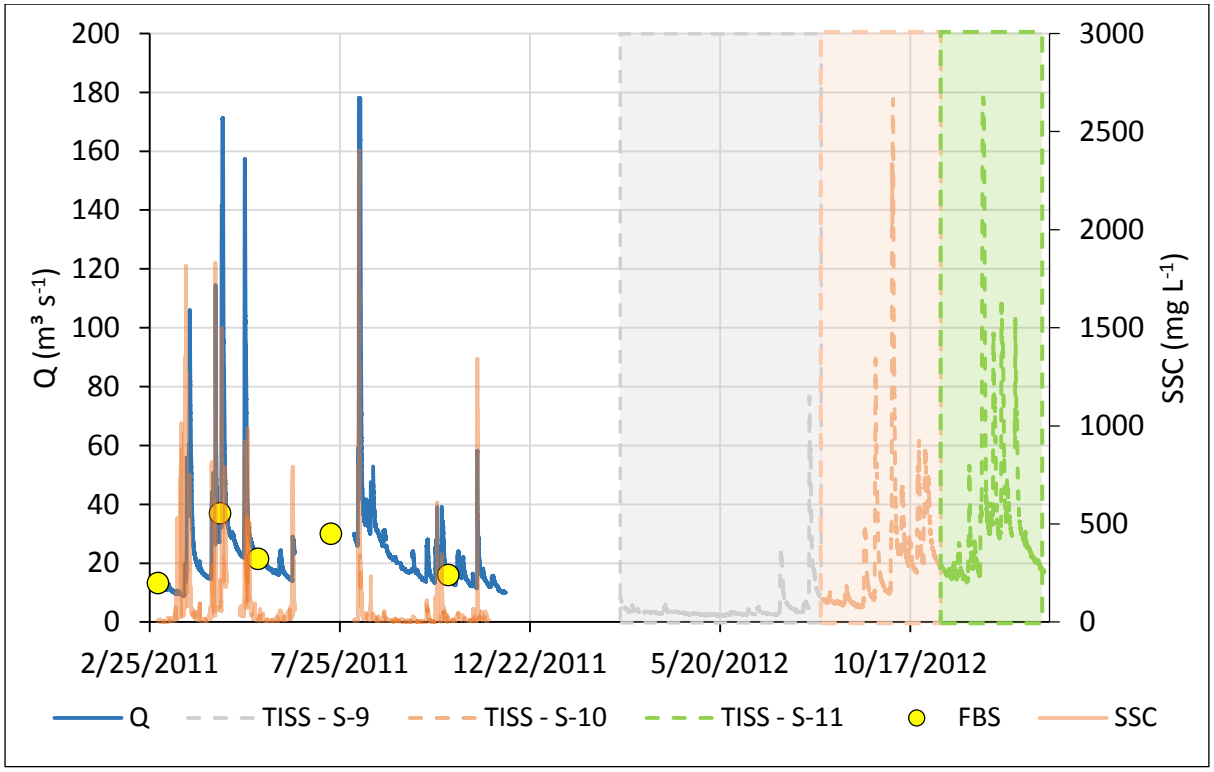
200
180
160
140
120
100
80
60
40
20
0
Q (m³ s⁻¹)
3000
2500
2000
1500
1000
500
0
SSC (mg L⁻¹)
2/25/2011
7/25/2011
12/22/2011
5/20/2012
10/17/2012
Q
TISS - S-9
TISS - S-10
TISS - S-11
FBS
SSC

Figure B1

Click here to download high resolution image

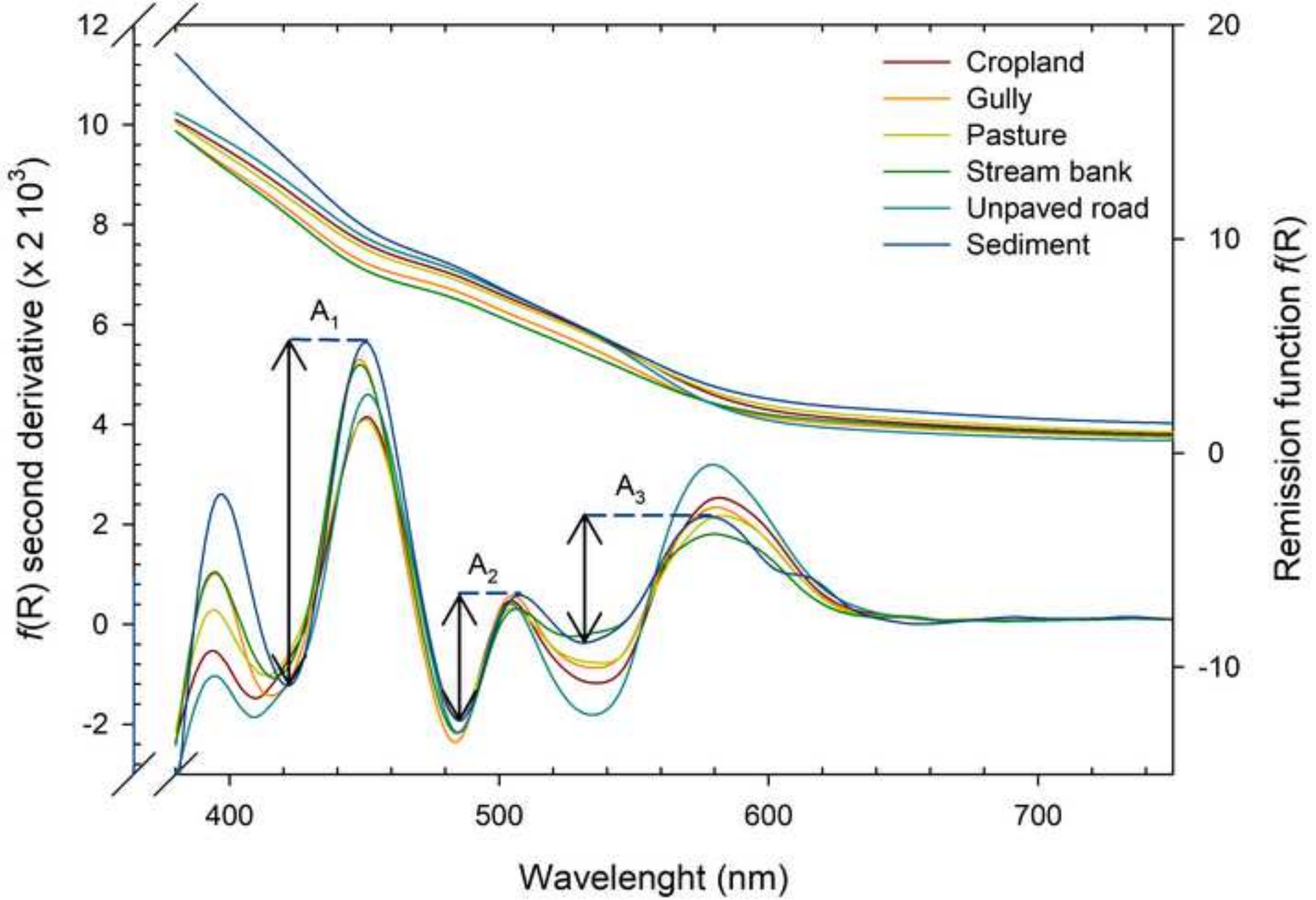

Figure captions

Figure 1. Location of the Conceição River catchment in Southern Brazil and digital elevation model.

Figure 2. Lithological formations, soil types and source sample location (a); and land use map for the year 2012 (b).

Figure 3. Correlation plot between variables that were approved in the conservativeness test and KW H test. The representation of the symbols " * " and " ' " used to differentiate the colour parameters was replaced by the letters "x" and "l" in the figure. xHF and xLF correspond to the magnetic parameters κ_{HF} and κ_{LF}, respectively.

Figure 4. Heat map and dendrogram of the variables that were approved in the conservativeness test and KW H test. The representation of the symbols " * " and " ' " used to differentiate the colour parameters was replaced by the letters "x" and "l" in the figure. xHF and xLF correspond to the magnetic parameters κ_{HF} and κ_{LF}, respectively.

Figure 5. Approach considering only UV-VIS derived parameters – UV. a) Source reclassification by the LDA using the selected variables. b) Box plot with the source contributions. The red cross point represents the mean, the horizontal line inside the box represents the median, the lower and upper edges of the box represent the 25th and 75th percentiles, whiskers represent the 10th and 90th percentiles, and circles represent values greater than the 90th percentile.

Figure 6. Approach considering the combination of UV and magnetic – MUV. a) Source reclassification by the LDA using the selected variables. b) Box plot with the source contribution. The red cross point represents the mean, the horizontal line inside the box represents the median, the lower and upper edges of the box represent the 25th

and 75th percentiles, whiskers represent the 10th and 90th percentiles, and circles represent values greater than the 90th percentile.

Figure 7. Approach considering the combination of GEO and UV parameters – GUV. a) Source reclassification by the LDA using the selected variables. b) Box plot with the source contribution. The red cross point represents the mean, the horizontal line inside the box represents the median, the lower and upper edges of the box represent the 25th and 75th percentiles, whiskers represent the 10th and 90th percentiles, and circles represent values greater than the 90th percentile.

Figure 8. Approach considering the combination of geochemical and magnetic parameters – GM. a) Source reclassification by the LDA using the selected variables. b) Box plot with the source contribution. The red cross point represents the mean, the horizontal line inside the box represents the median, the lower and upper edges of the box represent the 25th and 75th percentiles, whiskers represent the 10th and 90th percentiles, and circles represent values greater than the 90th percentile.

Figure 9. Mean contributions of each sediment source for the two types of sediment sampling strategies (TISS and FBS) and following the five approaches relying on different tracer combinations.

Figure A1. Water discharge (Q) and suspended sediment concentration (SSC) during the monitored period, sampling period of time integrated suspended sediment sampler (TISS) and sampling time of fine bed sediment samples (FBS).

Figure B1. Second-derivative spectra of the remission function *f*(R) from visible difuse reflectance spectroscopy showing the absorption bands (minima) of Fe-oxides in each landuse and sediment samples mean spectra.

47

Table 1
Click here to download Table: Table 1.docx

Table 1. Sediment samples and their respective period of sampling.

ID	Sample Type*	Collection period
S-1	FBS	02/03/2011
S-2	FBS	21/04/2011
S-3	FBS	21/05/2011
S-4	FBS	18/07/2011
S-5	FBS	18/10/2011
S-6	FBS	02/02/2012
S-7	FBS	24/03/2012
S-8	FBS	10/11/2012
S-9	TISS	02/03/2012 - 09/08/2012
S-10	TISS	17/08/2012 - 10/11/2012
S-11	TISS	10/11/2012 - 30/01/2013

*FBS – fine bed sediments and TISS – time integrated sediment samples.

Table 2
Click here to download Table: Table 2.docx

Table 2. Tracers removed by the conservative test.

Classical range test	IQR Approach
Co, V, Na, Ti, TOC, K, hvC	Al, Ba, Ca, Co, Cr, Cu, La, Li, Mg, Mn, Na, Ni, Sr, Ti, V, Zn, A1, A2, A3, a*, b*, CI, C*, G, h, HRGB, hvC, Hvc, IRGB, R, RI, SI, SRGB, u', u*, y, z

Table 3
Click here to download Table: Table 3.docx

Table 3. Selected tracers by the LDA for each tracer combination and the corresponding percentage of samples correctly classified (SCC).

Tracer combination	Tracers selected	% SCC
GEO	TOC, P, K	68.4%
UV	a, v*, v', b	59.4%
MUV	a, v*, v', b, χ_{HF}, χ_{LF}	60.4%
GUV	TOC, K, P, a, v*, b, L, L*	73.3%
GM	TOC, K, P, χ_{HF}, χ_{LF}	74.3%
GMUV	TOC, K, P, a, v*, b, L, L*	73.3%

G - geochemical tracers; UV – UV-VIS derived parameters; M - magnetic variables; SCC – Samples correctly classified.

Table 4
Click here to download Table: Table 4.docx

Table 4. Magnetic, geochemical and UV-VIS derived parameters concentrations in the potential sources and in sediment of the Conceição catchment, and results of the mean test.

Fingerprint property	Cropland	Pastures	Unpaved Road	Stream Banks	Gullies	Sources		Sediments	KW	
	Mean ± SD	Mean ± SD	Mean ± SD	Mean ± SD	Mean ± SD	Max	Min	Mean ± SD	p value	H value
n =	77	24	38	34	14	187		11		
□LF (10^{-6} m^3kg^{-1})	20.1 ± 8	15 ± 7.4	22 ± 8.7	11 ± 5.6	15.3 ± 9.3	42.7	1.7	14 ± 3	< 0.001	38.6
□HF (10^{-6} m^3kg^{-1})	18.4 ± 7.1	13.9 ± 6.8	19.4 ± 7.5	10.3 ± 5.2	13.7 ± 8	38.0	1.5	13.3 ± 3.1	< 0.001	36.7
TOC (g kg^{-1})	22 ± 4.6	25.9 ± 4.8	7.4 ± 4.6	15.7 ± 5.2	10.5 ± 5.9	36.3	1.5	22.4 ± 8.1	< 0.001	116.2
Ba (mg kg^{-1})	200.2 ± 84.6	209.7 ± 73.6	131.1 ± 79.4	215.1 ± 56.1	153.2 ± 72.2	500.4	46.1	261.9 ± 38.1	< 0.001	34.5
Be (mg kg^{-1})	3.7 ± 0.6	3.6 ± 0.7	3.5 ± 0.6	4 ± 0.6	3.5 ± 0.5	5.5	1.9	3.5 ± 0.6	0.010	13.2
Co (mg kg^{-1})	47 ± 21.6	53.3 ± 20.6	28.1 ± 18.8	59.6 ± 20.6	41.4 ± 30.5	118.8	2.6	88.5 ± 18.4	< 0.001	37.1
Cr (mg kg^{-1})	76.1 ± 19.1	77.8 ± 18.9	69.7 ± 14.5	79.8 ± 12.4	68.4 ± 26.3	146.4	39.4	88.4 ± 6.3	0.005	15.0
Cu (mg kg^{-1})	325.3 ± 66.8	306.3 ± 60.9	318.2 ± 73.1	335.2 ± 61.4	337.1 ± 77.5	568.2	139.3	303 ± 34	0.233	5.6
La (mg kg^{-1})	34.8 ± 10.1	31.8 ± 7.1	33.1 ± 10	37.6 ± 8.4	39.9 ± 7.5	66.8	15.8	30.6 ± 2.7	0.019	11.8
Li (mg kg^{-1})	56 ± 19.4	48.8 ± 22.2	73.1 ± 25.4	51.2 ± 12.4	63.2 ± 30.4	143.5	21.2	32.8 ± 3.5	< 0.001	24.4
Ni (mg kg^{-1})	50.1 ± 16.1	48.9 ± 12.8	53.3 ± 20.2	47.8 ± 11.9	41.7 ± 9.6	122.8	21.3	52.4 ± 2.3	0.240	5.5
Sr (mg kg^{-1})	23.9 ± 13	26.1 ± 11.8	13.7 ± 9.2	25.4 ± 8.6	22.4 ± 12.7	84.0	4.4	35 ± 5	< 0.001	55.2
V (mg kg^{-1})	365.3 ± 60.2	400.4 ± 70.4	299.7 ± 59.3	381.5 ± 60.4	309.5 ± 58.9	581.4	207.7	561.1 ± 87.5	< 0.001	48.9
Zn (mg kg^{-1})	13.8 ± 3.5	14.4 ± 3.5	12.2 ± 2.2	15.3 ± 3	11.9 ± 2.2	33.4	7.2	16.6 ± 2.8	< 0.001	25.7
Al (mg kg^{-1})	70578 ± 13882.3	59871.4 ± 11790.3	91786.4 ± 13002.7	61249.2 ± 10386.8	80320.9 ± 22155.4	113258.9	40415.3	50738.9 ± 4175.2	< 0.001	69.2
Ca (mg kg^{-1})	2140 ± 1204.3	2088.5 ± 1265.8	585.8 ± 904.3	1797.5 ± 838	1004.8 ± 1231	5423.2	0.0	3381 ± 697.6	< 0.001	67.1
Fe (mg kg^{-1})	92707.1 ± 12753.9	86542.5 ± 14868.8	89570.8 ± 11534.2	93838.2 ± 16710.6	90124.2 ± 9441.6	134108.4	48476.4	89629.6 ± 8526.4	0.219	5.7
K (mg kg^{-1})	928.9 ± 651.6	821.9 ± 679.9	697.1 ± 550.6	462.7 ± 384.7	535.3 ± 456.1	3392.3	79.7	397.5 ± 362	0.002	17.2
Mg (mg kg^{-1})	3142.8 ± 1591.8	3307.3 ± 1352.7	2182.8 ± 892.7	2985.9 ± 891	2875.6 ± 1712.4	8466.5	1239.0	3647.2 ± 360.6	< 0.001	26.9
Mn (mg kg^{-1})	1889 ± 580.1	2020.7 ± 746.1	1112.5 ± 546.1	2319.8 ± 1018.1	1739.7 ± 1039.4	5405.6	344.8	2880.2 ± 712.3	< 0.001	45.2
Na (mg kg^{-1})	77.4 ± 76.4	85.4 ± 71.1	78.2 ± 96.4	80.4 ± 35.8	60.6 ± 37.7	620.3	0.0	160.2 ± 170.7	0.163	6.5
P (mg kg^{-1})	486.9 ± 128.1	403.5 ± 66.2	300.8 ± 90.2	343.9 ± 147.7	256.2 ± 69.3	1104.6	59.7	467.7 ± 77.3	< 0.001	85.3
Ti (mg kg^{-1})	3091.8 ± 939	4176 ± 1045.5	2332.8 ± 738.8	3360.3 ± 931.3	2432.1 ± 678.6	6950.7	873.6	18662.4 ± 2472.2	< 0.001	49.2

L*	38.9 ± 3.3	38.3 ± 4.5	40.7 ± 4.8	41.2 ± 3.2	40.7 ± 5.7	52.5	23.8	37.1 ± 3.8	0.013	12.6
a*	16.4 ± 2.5	14.5 ± 2.7	21.5 ± 3.1	14.8 ± 2.5	17.3 ± 3.9	28.9	8.1	12.2 ± 1.5	< 0.001	72.1
b*	23.1 ± 2.2	21.6 ± 2.6	27.3 ± 3.2	24 ± 3.2	24.7 ± 4.2	36.7	15.4	21.5 ± 2.4	< 0.001	52.1
C*	28.4 ± 3.1	26.1 ± 3.6	34.7 ± 4.2	28.2 ± 3.8	30.2 ± 5.4	46.7	17.4	24.7 ± 2.8	< 0.001	60.8
h	54.7 ± 2.8	56.5 ± 3	51.9 ± 2.4	58.3 ± 2.9	55.4 ± 4	65.7	48.5	60.4 ± 1.2	< 0.001	69.0
x	0.4 ± 0	0.4 ± 0	0.5 ± 0	0.4 ± 0	0.4 ± 0	0.5	0.4	0.4 ± 0.006	< 0.001	56.1
y	0.4 ± 0	0.4 ± 0	0.4 ± 0	0.4 ± 0	0.4 ± 0	0.4	0.4	0.4 ± 0.005	< 0.001	42.5
z	0.2 ± 0	0.2 ± 0	0.2 ± 0	0.2 ± 0	0.2 ± 0	0.2	0.1	0.2 ± 0.007	< 0.001	54.7
L	32.6 ± 2.9	32.1 ± 3.9	34.2 ± 4.4	34.6 ± 2.9	34.3 ± 5.1	45.4	20.1	31.1 ± 3.3	0.013	12.7
a	12.5 ± 2.1	10.9 ± 2.3	16.9 ± 2.8	11.4 ± 2.1	13.4 ± 3.3	24.9	5.9	9 ± 1.4	< 0.001	69.2
b	12.3 ± 1.3	11.6 ± 1.6	14.2 ± 1.8	13.1 ± 1.7	13.3 ± 2.4	19.9	7.9	11.4 ± 1.5	< 0.001	37.6
u*	33.6 ± 4.8	29.9 ± 5.4	43.5 ± 6.3	32.1 ± 5.1	36 ± 7.8	62.3	17.9	26.4 ± 3.8	< 0.001	65.7
v*	21.8 ± 2.2	20.8 ± 2.8	24.7 ± 3	23.5 ± 3.1	23.5 ± 4.3	34.7	13.9	20.9 ± 2.8	< 0.001	32.8
u'	0.3 ± 0	0.3 ± 0	0.3 ± 0	0.3 ± 0	0.3 ± 0	0.3	0.2	0.3 ± 0	< 0.001	60.8
v'	0.5 ± 0	0.5 ± 0	0.5 ± 0	0.5 ± 0	0.5 ± 0	0.5	0.5	0.51 ± 0	< 0.001	65.4
RI	2.5 ± 1.5	3.5 ± 4.9	2.2 ± 1.2	1.8 ± 1	2.8 ± 4.1	25.8	0.5	3.1 ± 2.2	0.006	14.4
Hvc	163.7 ± 8.6	169.7 ± 9.7	152.3 ± 8.1	172.6 ± 8.1	164.2 ± 12.9	192.3	141.0	178.9 ± 3.3	< 0.001	71.5
hVc	23.4 ± 1.5	23.1 ± 2.1	24.2 ± 2.2	24.5 ± 1.4	24.3 ± 2.6	29.6	16.5	22.6 ± 1.7	0.013	12.7
hvC	30.0 ± 2.6	28.1 ± 3.1	35.2 ± 3.4	29.9 ± 3.0	31.6 ± 4.4	45.7	21.6	26.6 ± 2.6	< 0.001	60.8
R	193.5 ± 12.6	184.7 ± 14.0	216.1 ± 16.5	185.7 ± 12.3	196.8 ± 21.6	238.9	150.4	178.3 ± 4.9	< 0.001	60.2
G	74.8 ± 3.5	77.2 ± 3.6	68.7 ± 4.4	78.5 ± 3.2	74.5 ± 6.0	85.5	62.1	81 ± 1.1	< 0.001	70.2
B	34.2 ± 3.5	36.5 ± 4.1	28.1 ± 4.9	34.7 ± 4.2	32.8 ± 6.3	48.0	21.8	36.2 ± 1.9	< 0.001	53.5
HRGB	19.5 ± 4.1	16.7 ± 4.3	26.7 ± 5.2	15.8 ± 3.7	20.1 ± 6.9	34.1	7.5	13.1 ± 1.3	< 0.001	66.9
IRGB	100.8 ± 1.9	99.5 ± 2.2	104.3 ± 2.5	99.6 ± 1.9	101.3 ± 3.3	107.8	94.2	98.5 ± 0.8	< 0.001	60.2
SRGB	79.7 ± 8.0	74.1 ± 9.0	94.0 ± 10.6	75.5 ± 8.1	82.0 ± 13.8	108.3	51.2	71 ± 3.4	< 0.001	58.8
CI	0.44 ± 0.05	0.41 ± 0.05	0.52 ± 0.05	0.40 ± 0.04	0.45 ± 0.08	0.6	0.3	0.38 ± 0.02	< 0.001	64.7
SI	0.70 ± 0.04	0.67 ± 0.05	0.77 ± 0.05	0.68 ± 0.05	0.71 ± 0.08	0.8	0.5	0.66 ± 0.02	< 0.001	56.6
A1	0.003 ± 0.001	0.003 ± 0.002	0.004 ± 0.001	0.004 ± 0.002	0.004 ± 0.002	0.0	0.0	0.005 ± 0.001	< 0.001	19.9
A2	0.001 ± 0	0.001 ± 0.001	0.001 ± 0.001	0.001 ± 0.001	0.001 ± 0.001	0.0	0.0	0.002 ± 0.001	0.111	7.5
A3	0.002 ± 0.001	0.002 ± 0.001	0.003 ± 0.001	0.001 ± 0.001	0.002 ± 0.002	0.0	0.0	0.003 ± 0.001	< 0.001	51.0

SD – Standard Deviation

Table 5

Click here to download Table: Table 5.docx

Table 5. Mean contribution and mean standard deviation of each source contribution for all target sediment samples and for individual sediment sampling strategies conducted in the Conceição River catchment.

	Approaches	CR (%)			GU (%)			PA (%)			SB (%)			UR (%)		
		Mean	TISS	FBS	Mean	TISS	FBS	Mean	TISS	FBS	Mean	TISS	FBS	Mean	TISS	FBS
Source contribution	UV	16.6a	16.5b	16.7ab	15.9a	15.6a	16.0a	33.6a	34.7a	33.2a	31.2a	31.8ab	31.0a	2.6b	1.5b	3.1b
	GM	17.8a	24.3ab	15.4b	19.2a	10.7a	22.4a	24.4a	36.3a	19.9b	26.4a	23.2ab	27.7a	12.2a	5.5a	14.7a
	GUV	19.9a	32.5a	15.1b	17.0a	7.3a	20.6a	26.7a	40.5a	21.5ab	26.3a	16.8b	29.9a	10.1a	2.9a	12.8a
	MUV	23.1a	17.6ab	25.2a	14.4a	15.8a	14.0a	31.1a	32.3a	30.6ab	26.4a	31.5a	24.6a	4.9ab	2.9a	5.7ab
	GMUV	19.6a	32.6a	14.8b	17.1a	7.2a	20.8a	26.4a	40.3a	21.2ab	26.6a	17.1ab	30.2a	10.2a	2.8a	13.0a
Standard deviation	UV	31.7	31.8	31.6	29.5	29.2	29.7	38.2	38.6	38.0	36.9	37.2	36.9	9.5	7.5	10.2
	GM	26.7	26.9	26.7	29.7	19.6	33.5	30.9	31.8	30.6	34.5	27.9	37.0	23.9	13.4	27.8
	GUV	28.2	29.4	27.8	28.3	15.5	33.0	31.8	31.2	32.1	34.4	23.7	38.4	22.0	9.0	26.9
	MUV	28.1	29.5	27.6	28.3	15.5	33.1	31.7	31.2	31.8	34.5	23.9	38.5	22.0	8.6	27.0
	GMUV	30.4	27.4	31.5	24.6	26.1	24.1	32.9	34.1	32.5	31.3	34.0	30.2	12.3	10.1	13.1

*Means followed by the same letter in the columns do not differ statistically by the Kruskal-Wallis H-test at $p<0.05$. TISS = Time Integrated Sediment Sampler (n=3); FBS = Fine bed sediment samples from the river bottom (n=8); CR = Croplands; GU = Gullies, PA = Pastures; SB = Stream banks; and UR = Unpaved roads.